Full paper

Natural resolution of ill-posedness of inverse kinematics for redundant robots: a challenge to Bernstein's degrees-of-freedom problem

SUGURU ARIMOTO *, MASAHIRO SEKIMOTO, HIROE HASHIGUCHI
and RYUTA OZAWA

Department of Robotics, Ritsumeikan University, Kusatsu, Shiga 525-8577, Japan

Abstract—A robot designed to mimic a human becomes kinematically redundant, i.e. its total degrees of freedom becomes larger than the number of physical variables required for description of a given task. Kinematic redundancy may contribute to enhancement of dexterity and versatility, but incurs a problem of ill-posedness of inverse kinematics from the task-description space to the robot joint space. Such ill-posedness of inverse kinematics was originally found by A. N. Bernstein as the 'degrees-of-freedom problem' in physiology, who also pointed out the importance of unveiling the secret of the central nervous system in how nicely it coordinates a skeletomotor system with so many degrees of freedom interacting in complex ways. However, in the history of robotics research, such ill-posedness of inverse kinematics has not yet been tackled directly, but circumvented by introducing an artificial performance index and determining uniquely an inverse kinematics solution by minimizing it. This paper aims at challenging one of Bernstein's problems and proposes a new method for resolving such an ill-posedness problem in a natural way and in a dynamic sense without invoking any artificial performance index. Instead, a novel concept named 'stability on a manifold' is introduced and it is shown that there exists a sensory feedback signal from the task space to the joint space such that it enables the overall closed-loop dynamics to converge naturally and coordinately to a lower-dimensional manifold describing a set of joint states fulfilling a given motion task. This result is also extended by using the concept of 'transferability to a submanifold' in the case of short- or middle-range movement such as a task of multi-joint reaching.

Keywords: Redundancy resolution; redundant robots; Bernstein's problem; inverse kinematics; multi-joint reaching.

---

*To whom correspondence should be addressed. E-mail: arimoto@se.ritsumei.ac.jp

1. INTRODUCTION

If a robot is designed so as to mimic a human limb then its mechanism must be kinematically redundant, i.e. its total degrees of freedom becomes larger than the number of independent physical variables required for description of a given task. This kinematic redundancy contributes to enhancement of dexterity and versatility in execution of robot tasks, but incurs a problem of ill-posedness of inverse kinematics from the task-description space to the robot joint space. In order to eliminate such ill-posedness, many methods have been proposed, as surveyed in a special issue of the journal *Laboratory Robotics and Automation* [1], and a book specially dedicated to problems of redundancy and optimization [2]. Most of them are based on the idea of introducing some extra and artificial performance criterion for determining uniquely an appropriate joint space trajectory by minimizing it. In fact, examples of such performance indices in robotics research include: manipulability index [3], kinetic energy [4], quadratic norm of joint control torques [5], virtual fatigue function [6] and task-oriented priority using pseudoinverses [7−9]. Most proposed methods have been explicitly or implicitly based on the Jacobian pseudoinverse approach for planning an optimized joint velocity trajectory $\dot{q}(t)$ together with an extra term $(I - J^+(q)J(q))v$, where v is determined by optimizing the performance index, $J(q)$ is the Jacobian matrix of the task coordinates x with respect to the joint coordinates q and $J^+(q)$ is the pseudoinverse of $J(q)$. In the history of robot control the idea of using the pseudoinverse for generation of joint trajectories for redundant robots was initiated by Whitney [10] and analyzed in more detail by Liegeois [11]. Once a desired trajectory in the joint space is determined, it is claimed that the computed torque method can be applied for generating control signals to maneuver the robot to faithfully track the desired joint trajectory. In the case that an objective task x_d is given in the task space $x \in X$ and the computed torque method cannot be used due to uncertainties of kinematic parameters of the robot, a control signal u to be exerted through joint actuators of the robot is designed such as:

$$u = -C\dot{q} + J^\mathrm{T}(q)K(x(q) - x_\mathrm{d}) + \{I - J^+(q)J(q)\}v, \qquad (1)$$

where C is a constant positive definite matrix for damping shaping, K is a constant positive definite gain matrix and v is also determined so as to minimize an artificially introduced performance index.

On the other hand, the ill-posedness of inverse kinematics of a redundant system was originally pointed out by A. N. Bernstein as the 'degrees-of-freedom problem' in relation to human body movements [12, 13]. In particular, Bernstein was concerned very early on with the importance of unveiling the secret of the central nervous system that nicely coordinates a human skeltomotor system with so many degrees of freedom interacting with the 'real world' in complex ways. In fact, Murray *et al.* [14], quoting Hinton's article [15] dedicated to Bernstein's problems, claimed that 'The study of human biological motor mechanisms led the Russian psychologist Bernstein to question how the brain could control a system with so

many different degrees of freedom interacting in such a complex fashion. Many of these same complexities are also present in robotic systems and limit our ability to use multifingered hands and other robotic systems to their full advantage'. In physiology, most research works have been concerned with a simple, multi-joint reaching motion or pointing movement, (e.g., Refs [16–20]). Most of them are published in physiological journals and are more or less affected by the equilibrium point (EP) hypothesis of motor control posed by Feldman [21], equivalently observed by Bizzi *et al.* [17] as the spring-like effects of a group of muscles. This EP hypothesis can be interpreted in the control-theoretic language such that, for a specified arm endpoint x_d in Cartesian space, the central part of control for reaching it must be composed of the term $J^T(q)K(x - x_d)$ which corresponds to assuming introduction of an artificial potential $\Delta x^T K \Delta x / 2$ in the external world (task space), where $\Delta x = x - x_d$. In the case of redundant multi-joint reaching, however, there arises the same problem of ill-posedness of inverse kinematics. Thus, in parallel with the vast literature [1–11] in robotics research, many methods for elimination of redundancy of degrees of freedom have been proposed in the physiological literature initiated by Hogan [22]. Most of them are based on the introduction of extra performance criterion to be optimized: squared norm of joint jerks (rate of changes of acceleration) [18], energy [23], effort applied during movement [23], minimum torque [24] and minimum torque change [25, 26], although some of them are not used for redundancy resolution. Nevertheless, even all of the performance indices that lead successfully to unique determination of the inverse kinematics are not well-grounded physiologically and no physiological evidence or principle that associates such a performance index to generation of human movements could be found.

This paper aims at challenging one of Bernstein's problems, i.e. the problem of redundancy resolution of joint degrees of freedom for a simple multi-joint reaching motion. In the paper, we do not take into account the dynamics of muscles or joint actuators and therefore we assume that each joint torque can be exerted directly from its corresponding actuator. As a result, the joint control vector is set as:

$$u = -C\dot{q} - J^T(q)K(x(t) - x_d), \tag{2}$$

where C is a constant positive definite gain matrix for damping shaping, K is a constant gain matrix, x_d is a specified endpoint position vector in the task space and $x(t)$ is the measured position of the endpoint. The major difference between (1) and (2) is that the last term of (1) is missing in (2). This means that it is not necessary to solve the problem of inverse kinematics and use the pseudoinverse, but instead it is crucial to prove that appropriate choices of the gain matrices C and K render the system dynamics convergent as time elapses, i.e. $x(t) \rightarrow x_d$ and $\dot{q}(t) \rightarrow 0$ as $t \rightarrow \infty$. Since the system is redundant in degrees of freedom, the dimension of x is less than that of q. Therefore, the convergence of $x(t)$ to x_d does not imply the convergence of full $q(t)$. Instead, it is possible to show that $q(t)$ remains in a specified region such that the Jacobian matrix $J(q)$ is non-degenerated (of full

rank). In other words, the proposed control of (2) suggests that the problem of elimination of redundancy need not be solved, but can be ignored in the control of the dynamics. Alternatively, it can be said that a kind of physical principle for economies of skilled motions may work in the elimination of redundancy [27, 28]. This point will be discussed in more detail by referring to computer simulation results in the case of a multi-joint reaching motion.

In Section 2, a reaching task by a planar robot with four joints is introduced, and two concepts of 'stability on a manifold' and 'transferability to a submanifold' are explained which were originally introduced in the control of multi-fingered hands [29–32]. In Section 3, local stability of an equilibrium state when the endpoint position is specified at $x = x_d$ is proved on the basis of the concept of stability on a manifold. In Section 4, asymptotic stability of the global reaching motion is proved on the basis of the concept of transferability to a submanifold. In Section 5, a variety of computer simulation results are presented which show the importance of gain tunings for damping factors and stiffness parameters of a hypothesized potential of the endpoint. A guidance of better tuning of feedback gains is suggested through the convergence analysis of the closed-loop dynamics and those simulation results. In the final section before the Conclusions some physiological implications and physical principles underlying the proposed control method and the results obtained in the paper are discussed.

2. CLOSED-LOOP DYNAMICS OF MULTI-JOINT REACHING MOVEMENT

Lagrange's equation of motion of a multi-joint system whose motion is confined to a plane as shown in Fig. 1 is described by the formula (see Ref. [33]):

$$H(q)\ddot{q} + \left\{ \frac{1}{2}\dot{H}(q) + S(q, \dot{q}) \right\} \dot{q} = u, \tag{3}$$

where $q = (q_1, q_2, q_3, q_4)^T$ denotes the vector of joint angles, $H(q)$ is the inertia matrix, and $S(q, \dot{q})\dot{q}$ is the gyroscopic force term including centrifugal and Coriolis force. It is well known that the inertia matrix $H(q)$ is symmetric and positive definite, and there exist positive constants h_m and h_M together with a positive definite constant matrix H_0 such that:

$$h_m H_0 \leqslant H(q) \leqslant h_M H_0 \quad \text{and} \quad 0 < H_0 \leqslant I, \tag{4}$$

for any q. It should be also noted that $S(q, \dot{q})$ is skew symmetric and linear, and homogeneous in $\dot{q}$. Any entry of $H(q)$ and $S(q, \dot{q})$ is constant or a sinusoidal function of components of q.

For a given specified target position $x_d = (x_d, y_d)^T$ as shown in Fig. 1, if the control input of (2) is used at joint actuators then the closed-loop equation of motion of the system can be expressed as:

$$H(q)\ddot{q} + \left\{ \frac{1}{2}\dot{H}(q) + S(q, \dot{q}) + C \right\} \dot{q} + J^T(q)K\Delta x = 0, \tag{5}$$
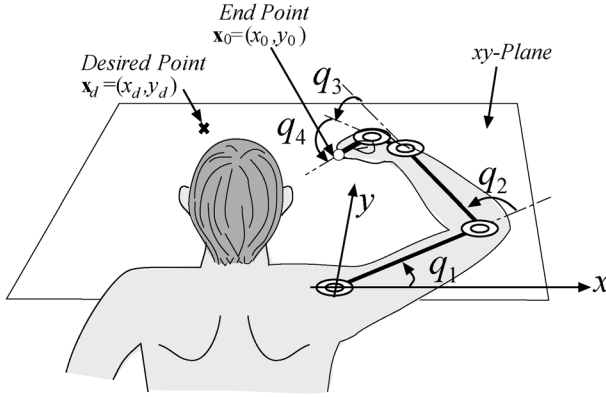
Figure 1. 'Reaching' by means of a surplus degrees of freedom system of hand–arm dynamics.

which follows from substitution of (2) into (3), where $\Delta x = x - x_{\mathrm{d}}$. Since $\dot{x} = J(q)\dot{q}$, the inner product of (5) with $\dot{q}$ is reduced to:

$$\frac{\mathrm{d}}{\mathrm{d}t}E = -\dot{q}^{\mathrm{T}}C\dot{q}, \tag{6}$$

where E stands for the total energy, i.e.:

$$E(q, \dot{q}) = \frac{1}{2}\dot{q}^{\mathrm{T}}H(q)\dot{q} + \frac{1}{2}\Delta x^{\mathrm{T}}K\Delta x. \tag{7}$$

Evidently the first term of this quantity E stands for the kinetic energy of the system. In this paper, the second term is called an artificial potential that appears due to addition of equilibrium point feedback control $J^{\mathrm{T}}(q)K\Delta x$ based on the error Δx expressed in Cartesian space. As is well known in robot control (see Ref. [33]), the relation of (6) denotes passivity of the closed-loop dynamics of (5). It also reminds us of Lyapunov's stability analysis, since it shows that the derivative of a scalar function E in time t is negative semi-definite. However, it should be noted that the scalar function $E(q, \dot{q})$ is not positive definite with respect to the state vector $(q, \dot{q}) \in R^8$. In fact, E includes only a quadratic term of two-dimensional (2D) vector Δx except the kinetic energy as a positive definite quadratic function of $\dot{q}$. Therefore, it is natural and reasonable to introduce a 2D manifold defined as:

$$M_2 = \{(q, \dot{q}) : E(q, \dot{q}) = 0 \ (\dot{q} = 0, x(q) = x_{\mathrm{d}})\},$$

which we call the equilibrium-point manifold. Next, consider a posture $(q^0, 0)$ with still state (i.e. $\dot{q} = 0$) whose endpoint is located at x_{d} as is shown in Fig. 2 by 'A)', i.e. $x(q^0) = x_{\mathrm{d}}$ and hence $(q^0, 0) \in M_2$, and analyze stability of motion of the closed-loop dynamics in a neighborhood of this equilibrium state. This equilibrium point in R^8 and belonging to M_2 is called the reference equilibrium state in this paper.
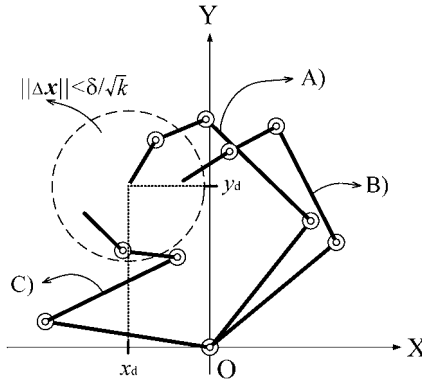
Figure 2. Target and initial postures of the arm-hand system: 'A)' stands for the reference state with joint position q^0, 'B)' is an initial state inside $N^8(\delta, r)$ with $\|q(0) - q^0\| < r$ and 'C)' is a state outside $N^8(\delta, r)$ because $\|q(0) - q^0\| > r$.
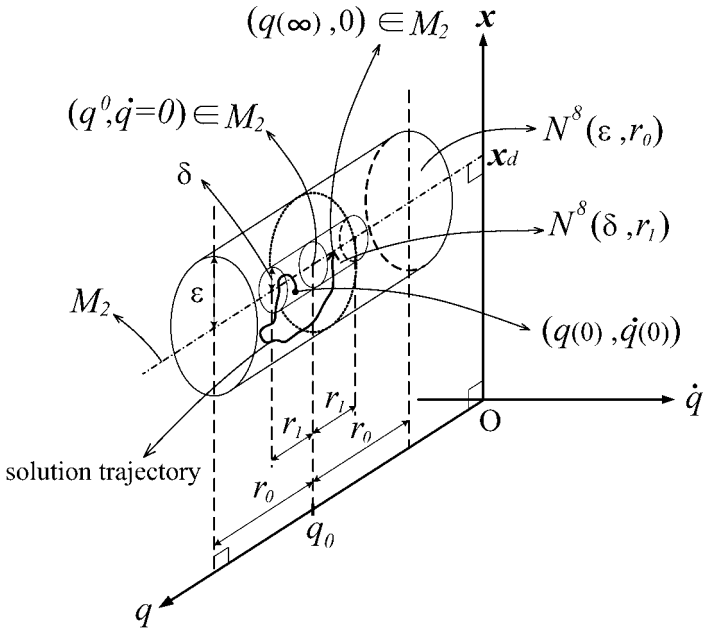
Figure 3. Definitions of 'stability on a manifold' and 'transferability to a submanifold'.

It is now necessary to introduce the concept of neighborhoods of the reference equilibrium state $(q^0, 0) \in M_2$ in R^8, which are conveniently defined with positive parameters $\delta > 0$ and $r_0 > 0$ as:

$$N^8(\delta, r_0) = \left\{ (q, \dot{q}) : E(q, \dot{q}) \leqslant \delta^2 \text{ and } \|q - q^0\|_K \leqslant r_0 \right\},$$

where $\|q - q^0\|_K = \{(1/2)(q - q^0)^T H(q)(q - q^0)\}^{1/2}$ (see Fig. 3). The necessity of imposing the inequality condition $\|q - q^0\|_K \leqslant r_0$ comes from avoiding possible movements arising such as self-motion [34] due to redundancy of degrees

of freedom far from the original posture. In fact, for the given endpoint x_d with the reference state as shown 'A)' in Fig. 2, one possible state with posture 'B)' in Fig. 2 may be inside $N^8(\delta, r_0)$, but another state 'C)' must be excluded from the neighborhood $N^8(\delta, r_0)$ by choosing $r_0 > 0$ appropriately, because the overall posture of 'C)' deviates by far from that of the original reference equilibrium state $(q^0, 0)$. Further, it is necessary to assume that the reference equilibrium state $(q^0, 0)$ is considerably distant from the posture that has singularity of the Jacobian matrix $J(q)$. Since (x, y) can be expressed as:

$$\begin{cases} x = l_1 \cos q_1 + l_2 \cos(q_1 + q_2) + l_3 \cos(q_1 + q_2 + q_3) \\ \quad + l_4 \cos(q_1 + q_2 + q_3 + q_4) \\ y = l_1 \sin q_1 + l_2 \sin(q_1 + q_2) + l_3 \sin(q_1 + q_2 + q_3) \\ \quad + l_4 \sin(q_1 + q_2 + q_3 + q_4), \end{cases} \tag{8}$$

the Jacobian matrix can be expressed as:

$$J(q) = \begin{pmatrix} -y & -y + l_1 s_1 & -y + l_1 s_1 + l_2 s_{12} & -y + l_1 s_1 + l_2 s_{12} + l_3 s_{123} \\ x & x - l_1 c_1 & x - l_1 c_1 - l_2 c_{12} & x - l_1 c_1 - l_2 c_2 - l_3 c_{123} \end{pmatrix}, \tag{9}$$

where l_i denotes the length of link i for $i = 1, 2, 3$ and 4, and $\sin(q_1) = s_1$, $\sin(q_1 + q_2) = s_{12}$, $\cos(q_1 + q_2) = c_{12}$, etc. It is easy to check that the Jacobian matrix $J(q)$ is of full rank (non-degenerated) except the case that $q_2 = q_3 = q_4 = 0$ in the range of $|q_i| < \pi$ for $i = 1, \ldots, 4$, which corresponds to the posture when the arm is stretched straight forward. Thus, we reasonably assume that $J(q)$ is of full rank in $N^8(\delta, r_0)$, and there exist constants $\lambda_m > 0$ and $\lambda_M > 0$ such that:

$$\begin{aligned} \lambda_m I_2 &\leqslant \min_{q \in N^8(\delta, r_0)} \lambda_m(J(q)J^T(q)) \\ &\leqslant \max_{q \in N^8(\delta, r_0)} \lambda_M(J(q)J^T(q)) \leqslant \lambda_M I_2, \end{aligned} \tag{10}$$

where $\lambda_m(X)$ or $\lambda_M(X)$ denote the minimum or maximum eigenvalue of X, respectively.

We are now in a position to define the concept of stability of the reference equilibrium state lying on the manifold M_2.

DEFINITION 1. If for an arbitrarily given $\varepsilon > 0$ there exist a constant $\delta > 0$ depending on ε and another constant $r_1 > 0$ independent of ε and less than r_0 such that a solution trajectory $(q(t), \dot{q}(t))$ of the closed-loop dynamics of (5) starting from any initial state $(q(0), \dot{q}(0))$ inside $N^8(\delta(\varepsilon), r_1)$ remains in $N^8(\varepsilon, r_0)$, then the reference equilibrium state $(q^0, 0)$ is called stable on a manifold (see Fig. 3).

DEFINITION 2. If for a reference equilibrium state $(q^0, 0) \in R^8$ there exist constants $\varepsilon_1 > 0$ and $r_1 > 0$ $(r_1 < r_0)$ such that any solution of the closed-loop dynamics of (5) starting from an arbitrary initial state in $N^8(\varepsilon_1, r_1)$ remains in $N^8(\varepsilon_1, r_0)$ and converges asymptotically as $t \to \infty$ to some point on $M_2 \cap N^8(\varepsilon_1, r_0)$, then the neighborhood $N^8(\varepsilon_1, r_1)$ of the reference equilibrium state $(q^0, 0)$ is said to be transferable to a submanifold of M_2.

This definition means that, even if a still state $(q^0, 0) \in M_2$ of the multi-joint system is forced to move instantly to a different state $(q(0), \dot{q}(0))$ in the neighborhood of $(q^0, 0)$ due to some external disturbance, the sensory feedback control of (2) assures that the system's state soon recovers to another still state $(q^\infty, 0) \in M_2 \cap N^8(\varepsilon_1, r_0)$ whose endpoint attains the original point $x(q^\infty) = x_d$, although the convergent posture q^∞ possibly differs from the original one q^0, but remains within $\|q^\infty - q^0\|_K \leqslant r_0$.

3. STABILITY OF MOTION IN THE NEIGHBORHOOD OF THE EQUILIBRIUM STILL STATE

Consider now stability on a manifold in a neighborhood of the reference still state $(q^0, 0)$ for a robotic arm with 4 d.o.f. as shown in Fig. 2. Link lengths and link inertia moments are shown as in Table 1, which are chosen on the basis of average human adult data. Note that inertia moments of a circular link with mass m and length l are of the order of $ml^2/12$ to $ml^2/3$ depending on the locations of the rotational center and axis. This means that inertia moments of the robot or human fingers become quite small and actually of the order of 10^{-6} to 10^{-7} kgm^2. In this case, if the damping coefficient c_i for finger joint i is chosen to be of the order 10^{-3} to 10^{-2} kgm^2/s for all i depending on the object mass, then non-linear terms composed of centrifugal and coriolis forces in the Lagrange equation can be treated to be negligibly small relative to inertia terms and other constraint force terms as discussed in previous papers [29–32]. Differently from the case of fingers, inertia moments of the human arm together with the hand are far larger than those of human fingers, but even the inertia moment of an upper arm of human adults remains to be $O(10^{-2})$ kgm^2 as shown in Table 1. In this case, the choice of damping coefficients c_i for joint i ($i = 1, 2, 3$ and 4 refer to joints of the shoulder, elbow, wrist and third (root) joint of index finger) is quite sensitive to the effects of non-linear terms including centrifugal and coriolis forces.

Now, for a given $\varepsilon > 0$, choose $r_1 < r_0$ and $\delta_1 \leqslant \varepsilon$ appropriately, and assume that an arbitrary initial condition $(q(0), \dot{q}(0))$ is lying in $N^8(\delta_1, r_1)$. Then, according to (6), the solution $(q(t), \dot{q}(t))$ of the closed-loop dynamics of (5) starting from the

Table 1.
Link lengths and inertia moments

Arm and hand	Link length (m)	Inertia moment (kgm^2)	Mass (kg)
Upper arm	$l_1 = 0.3$	$I_1 = 4.584 \times 10^{-2}$	$m_1 = 1.508$
Forearm	$l_2 = 0.27$	$I_2 = 1.872 \times 10^{-2}$	$m_2 = 0.7634$
Palm	$l_3 = 0.1$	$I_3 = 6.852 \times 10^{-4}$	$m_3 = 0.1963$
Index finger	$l_4 = 0.1$	$I_4 = 1.055 \times 10^{-4}$	$m_4 = 0.03141$

initial state $(q(0), \dot{q}(0))$ satisfies:

$$E(q(t), \dot{q}(t)) \leqslant \delta_1^2 \leqslant \varepsilon^2. \tag{11}$$

Therefore, it only remains to prove that the position state $q(t)$ does not go far from $q(0)$ and q^0, and remains inside of the sphere $S = \{q : \|q(t) - q^0\|_K^2 < r_0^2\}$ if $r_1 > 0$ and $\delta_1 > 0$ are appropriately chosen. However, we need to emphasize that to prove this is not a trivial task because the scalar function E is not positive definite in q or $q - q(0)$, as pointed out previously. Therefore, it is necessary to introduce a modified scalar function defined as:

$$V(q, \dot{q}) = E(q, \dot{q}) + \alpha \dot{q}^T H(q) J^T(q) K \Delta x, \tag{12}$$

where $\alpha > 0$ is a constant determined later. Then, the derivative of (12) in time t leads to:

$$\begin{aligned}
\dot{V} &= \dot{E} + \alpha \ddot{q}^T H J^T K \Delta x \\
&\quad + \alpha \dot{q}^T \left\{ (\dot{H} J^T + H \dot{J}^T) K \Delta x + H J^T K J \dot{q} \right\} \\
&= -\dot{q}^T C \dot{q} - \alpha \Delta x^T K J J^T K \Delta x - \alpha \dot{q}^T C J^T K \Delta x \\
&\quad + \alpha \dot{q}^T \left\{ \left(\frac{1}{2} \dot{H} J^T + H \dot{J}^T + S J^T \right) K \Delta x + H J^T K J \dot{q} \right\}. \tag{13}
\end{aligned}$$

In what follows, we set $K = k I_2$ (I_2 denotes the 2×2 identity matrix) and note that:

$$-\alpha \dot{q}^T C J^T K \Delta x \leqslant \frac{\alpha}{2} \dot{q}^T C^2 \dot{q} + \frac{\alpha k^2}{2} \Delta x^T J J^T \Delta x. \tag{14}$$

Then, by substituting this inequality into (13), (13) is reduced to:

$$\begin{aligned}
\dot{V} &\leqslant -\dot{q}^T C \left(I_2 - \frac{\alpha}{2} C \right) \dot{q} \\
&\quad - \frac{\alpha k^2}{2} \Delta x^T J J^T \Delta x + \alpha k h(\dot{q}, \Delta x), \tag{15}
\end{aligned}$$

where

$$h(\dot{q}, \Delta x) = \dot{q}^T \left\{ \left(\frac{1}{2} \dot{H} J^T + H \dot{J}^T + S J^T \right) \Delta x + H J^T J \dot{q} \right\}. \tag{16}$$

It is important to evaluate the last term $\alpha k h(\dot{q}, \Delta x)$ of the right-hand side of (15). Since $\dot{H}$, $\dot{J}$ and $S(q, \dot{q})$ are linear and homogeneous in components of vector $\dot{q}$, it is possible to show that there exists a positive constant r_0 such that:

$$|h(\dot{q}, \Delta x)| \leqslant \dot{q}^T \bar{C} \dot{q} \sigma_M \|\Delta x\| + \dot{q}^T H(q) \dot{q} (\sigma_M \|\Delta x\| + \lambda_M), \tag{17}$$

where σ_M stands for the maximum spectral radius of $J(q)$ in $N^8(\delta_1, r_0)$, $\bar{C} = \text{diag}(\bar{c}_1, \bar{c}_2, \bar{c}_3, \bar{c}_4)$ and $\bar{c}_i > 0$ for all $i = 1$ to 4 are at most of $O(10^{-1})$ as discussed more precisely in Appendix A. Since $k \|\Delta x\|^2/2$ is upper-bounded by $E(q(0), \dot{q}(0)) \leqslant \delta_1^2$ according to (6), it follows that $\|\Delta x\| < \sqrt{2/k} \delta_1$. The maximum spectral radius σ_M of $J(q)$ may also be evaluated as discussed in

Table 2.
Inertia matrix at initial posture with $q(0) = [45.0, 70.0, 60.0, 50.0]^T$ (deg)

$$H(0) = \begin{vmatrix} 0.20272 & 0.053757 & -5.9019 \times 10^{-5} & -0.00040982 \\ 0.053757 & 0.039842 & 0.0029112 & 6.1423 \times 10^{-5} \\ -5.9019 \times 10^{-5} & 0.0029112 & 0.0013068 & 0.00020648 \\ -0.00040982 & 6.1423 \times 10^{-5} & 0.00020648 & 0.00010551 \end{vmatrix}$$

Appendix B and it is concluded that, in the case of an admissible initial state as shown in Fig. 2, $\sigma_M \leqslant 0.5$. On the other hand, by choosing an appropriate $r_0 > 0$ it is possible to assume a positive constant $\lambda_m > 0$ such that for any $(q, \dot{q}) \in N(\delta_1, r_0)$ it holds that:

$$J(q)J^T(q) \geqslant \lambda_m I_2, \tag{18}$$

because any singular still states $(q^*, 0)$ satisfying $\det J(q^*)J^T(q^*) = 0$ arise if and only if $q_2 = q_3 = q_4 = 0$ and any permissible initial states whose endpoints lie inside the circle indicated in Fig. 2 are far distant from any singular still states in the joint space. In reality, in the case of Fig. 2, λ_m can be evaluated by numerical computation on the basis of physical parameters of the arm–hand system as $\lambda_m > 0.075$. Thus, $\dot{V}$ of (15) is reduced to:

$$\dot{V} \leqslant -\dot{q}^T C \left(I_4 - \frac{\alpha}{2} C \right) \dot{q} - \frac{\alpha \lambda_m k}{2} k \| \Delta x \|^2$$
$$+ \alpha k \sqrt{\frac{1}{2k}} \delta_1 \dot{q}^T \bar{C} \dot{q} + \alpha k \left(\sqrt{\frac{1}{2k}} \delta_1 + \lambda_M \right) \dot{q}^T H(q) \dot{q}. \tag{19}$$

Now, it should be remarked that damping factors c_i for joint i $(i = 1, \ldots, 4)$ must be chosen carefully in accordance with the inertia matrix $H(q)$ at the initial position $q(0)$, the magnitude of k $(K = kI_2)$ specifying the magnitude of artificial potential $k\|\Delta x\|^2/2$ in (7) and the corresponding ith component J_i^T of $J^T(q) = (J_1, J_2, J_3, J_4)^T$ $(i = 1, \ldots, 4)$. Since $H(q(0))$ $(= H(0))$ at the initial position corresponding to the position expressed by 'B' in Fig. 2 is given as in Table 2 and λ_m is bounded from below as $\lambda_m \geqslant 0.075$, one of the good choices for k and c_i is as follows:

$$k = 8.0 \quad \text{and} \quad c_1 = 1.0, \quad c_2 = 0.6, \quad c_3 = 0.1 \quad \text{and} \quad c_4 = 0.04. \tag{20}$$

Actually, computer simulation results show that, on the basis of choice for dampings c_i of (20), endpoint trajectories (x, y) of the closed-loop dynamics of (5) starting from the position $(q_1, q_2, q_3, q_4) = (45, 70, 60, 50)$ (deg) attain the best performance around $k = 7.5$–8.0 as shown in Figs 4–7. In what follows, we set $k = 8.0$. From these data together with (20), it is reasonable to assume (see (A.3) in Appendix A) that:

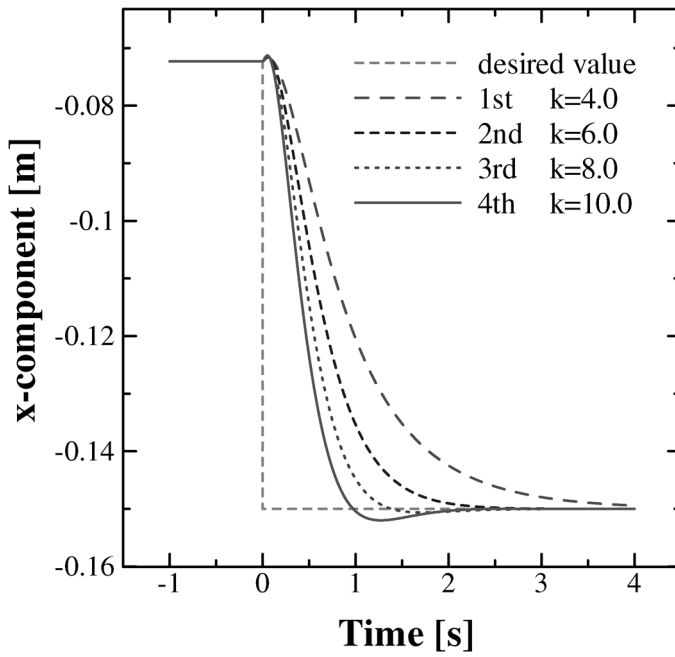$$C > 4 \left(H(q) + \frac{2}{7} \bar{C} \right), \tag{21}$$
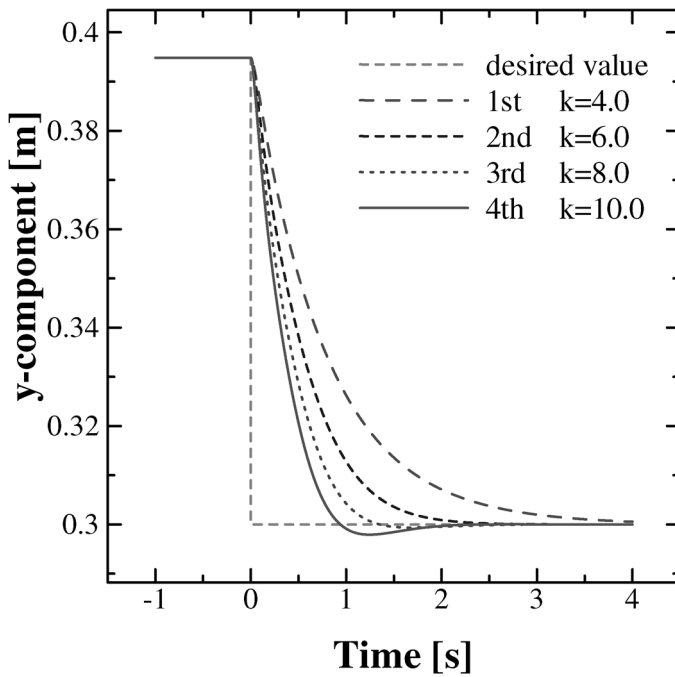
Figure 4. Transient responses of x for various k.

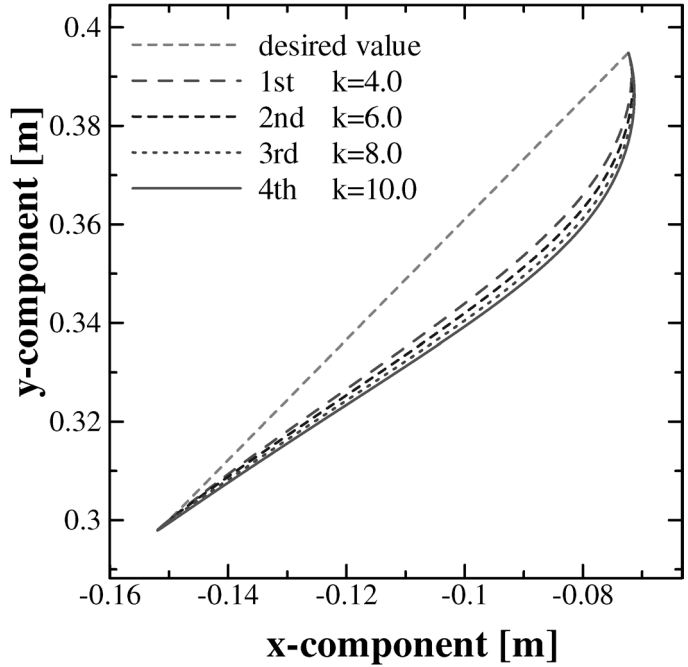**Figure 5.** Transient responses of y for various k.

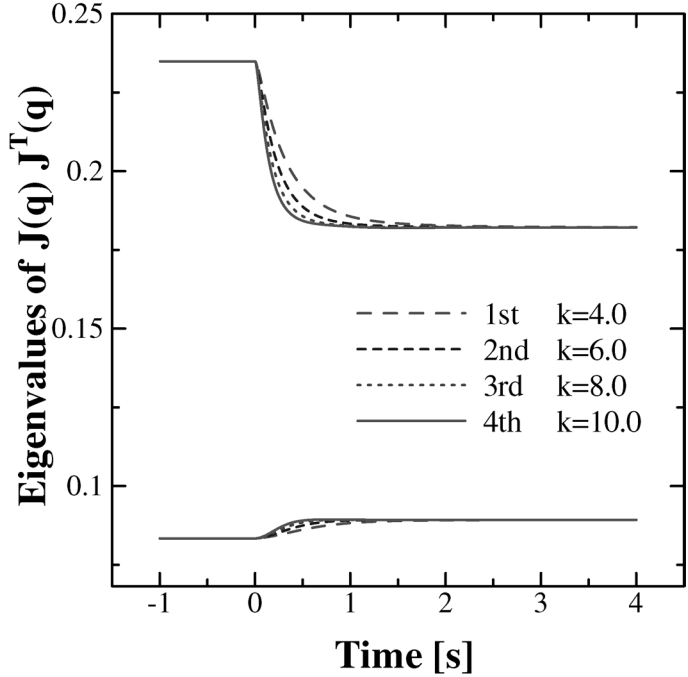**Figure 6.** Transient response of the robot endpoint in the xy-plane.

Figure 7. Transient responses of two eigenvalues of $J(q)J^{T}(q)$ for various k.

for all q along the solution trajectory to (5). Then, (19) can be reduced to:

$$\dot{V} \leqslant -\dot{q}^{\mathrm{T}} C \left(\frac{3}{8} I_4 - \frac{\alpha}{2} C \right) \dot{q} - \frac{9}{160} \dot{q}^{\mathrm{T}} C \dot{q} - \frac{9}{20} \cdot \frac{k}{2} \| \Delta x \|^2$$

$$- \frac{91}{160} \dot{q}^{\mathrm{T}} C \dot{q} + 2\alpha \delta_1 \dot{q}^{\mathrm{T}} \bar{C} \dot{q} + 2\alpha (\delta_1 + 4\lambda_{\mathrm{M}}) \dot{q}^{\mathrm{T}} H(q) \dot{q}. \qquad (22)$$

Further, if $\| x(0) - x_{\mathrm{d}} \| \leqslant 0.2$, then δ_1 can be set as $\delta_1 \leqslant 0.4$. Thus, by choosing $\alpha = 3/4$ and noting that $\lambda_{\mathrm{M}} \leqslant \sigma_{\mathrm{M}}^2 \leqslant 0.25$, it is possible to see from (21) that:

$$\dot{V} \leqslant -\frac{9}{20} E(x, \dot{x}). \qquad (23)$$

Next, note that

$$V = \frac{1}{2} \dot{q}^{\mathrm{T}} H(q) \dot{q} + \frac{k}{2} \| \Delta x \|^2 + \alpha \dot{q}^{\mathrm{T}} H(q) J^{\mathrm{T}}(q) k \Delta x$$

$$\geqslant \frac{1}{2} \dot{q}^{\mathrm{T}} H(q) \dot{q} + \frac{k}{2} \| \Delta x \|^2 - \frac{\alpha \gamma}{2} \dot{q}^{\mathrm{T}} H^2(q) \dot{q}$$

$$- \frac{\alpha k^2}{2\gamma} \Delta x^{\mathrm{T}} J J^{\mathrm{T}} \Delta x$$

$$\geqslant (1 - \alpha \gamma h_{\mathrm{M}}) \frac{1}{2} \dot{q}^{\mathrm{T}} H(q) \dot{q} + \left(1 - \frac{\alpha k \lambda_{\mathrm{M}}}{\gamma} \right) \frac{k}{2} \| \Delta x \|^2, \qquad (24)$$

where $\gamma > 0$ is an arbitrary constant. Since $h_{\mathrm{M}} \leqslant 0.222$ and $\lambda_{\mathrm{M}} \leqslant 0.25$, by choosing $\gamma = 3.0$, (24) can be reduced to:

$$V \geqslant \left(1 - \frac{2}{3}\alpha \right) \frac{1}{2} \dot{q}^{\mathrm{T}} H(q) \dot{q} + \left(1 - \frac{2}{3}\alpha \right) \frac{k}{2} \| \Delta x \|^2, \qquad (25)$$

which, by setting $\alpha = 3/4$, can be reduced to:

$$V(\Delta x, \dot{q}) \geqslant \frac{1}{2} E(\Delta x, \dot{q}), \qquad (26)$$

and similarly:

$$V(\Delta x, \dot{q}) \leqslant \frac{3}{2} E(\Delta x, \dot{q}). \qquad (27)$$

We are now in a position to state the main result of the paper in the following theorem:

THEOREM 1. *For a given reference still state* $(q^0, 0)$ *as shown in* Fig. 2 (*marked as 'A'*) *for the closed-loop dynamics of* (5) *with physical parameters of* Table 1, *and damping factors* c_i *and positioning feedback gain* k $(K = kI_2)$ *defined in* (20), *if there are positive constants* $\delta_1 > 0$ *and* $r_0 > 0$ *such that inequality* (18) *holds with* $\lambda_{\mathrm{m}} = 0.075$ *and* $\lambda_{\mathrm{M}} = 0.25$ *in* $N^8(\delta_0, r_0)$, *then the reference state* $(q^0, 0)$ *is stable on a manifold, and furthermore there exist positive constants* $\varepsilon_1 > 0$ *and* $r_1 > 0$ *such that the neighborhood* $N^8(\varepsilon_1, r_1)$ *is transferable to a submanifold of* M_2.

Proof. For an arbitrarily given $\varepsilon > 0$, choose $\delta(\varepsilon)$ so that $\delta(\varepsilon) = \min\{r_0/3, \delta_1\}$ if $\varepsilon > r_0$ and $\delta(\varepsilon) = \min\{\varepsilon/3, \delta_1\}$ otherwise. Since in this theorem we are concerned with stability in the vicinity of $(q^0, 0)$, we restrict the range of $x(0)$ such that $\|x(0) - x_d\| < 0.2$. This implies that $(q(0), \dot{q}(0)) \in N^8(\delta_1, r_1)$ with $\delta_1 \leqslant 0.4$ and some appropriate $r_1 > 0$. Therefore, in what follows, we reasonably assume that $\delta_1 \leqslant 0.4$. Then, inequalities (23), (26) and (27) follow as discussed above. Further, it should be noted that:

$$\dot{V} + \gamma(V - E) = -\dot{q}^T C \dot{q} - \alpha k^2 \Delta x^T J J^T \Delta x \\ - \alpha k \dot{q}^T (C - \gamma H) J^T \Delta x + \alpha k h(\dot{q}, \Delta x), \quad (28)$$

the right-hand side of which differs from that of (13) only in the third term, where C is replaced with $C - \gamma H \geqslant 0$ if γ is set as $\gamma = 9/20$. Then, applying the same argument developed above by applying a similar inequality to (14) where C is replaced with $C - \gamma H$ with $\gamma = 9/20$, we obtain:

$$\dot{V} + \frac{9}{20}(V - E) \leqslant -\frac{9}{20}E. \quad (29)$$

This is equivalent to:

$$\dot{V} \leqslant -(9/20)V, \quad (30)$$

which means:

$$E(\Delta x(t), \dot{q}(t)) \leqslant 2V(\Delta x(t), \dot{q}(t)) \\ \leqslant 2V(\Delta x(0), \dot{q}(0))e^{-(9/20)t} \\ \leqslant 3E(\Delta x(0), \dot{q}(0))e^{-(9/20)t}. \quad (31)$$

For simplicity, denote $E(\Delta x(t), \dot{q}(t))$ by $E(t)$. Then, any solution $(q(t), \dot{q}(t))$ to the closed-loop dynamics of (5) starting from $(q(0), \dot{q}(0))$ inside $N^8(\delta(\varepsilon), r_1)$ with some $r_1 > 0$ such that $r_0 \geqslant r_1 > 0$ (the value for r_1 will be determined later) satisfies:

$$E(\Delta x(t), \dot{q}(t)) \leqslant 3\delta^2(\varepsilon)e^{-(9/20)t}. \quad (32)$$

This means that all $\dot{q}(t)$ and $\Delta x(t)$ converge to zero exponentially in t. Hence, from (5) it follows that all $\ddot{q}(t)$ converge to zero exponentially in t, too. Then, by taking the integral of (5) over $t \in [0, t)$, it follows that:

$$C(q(t) - q(0)) \\ = -\int_0^t \left(H\ddot{q} + \frac{1}{2}\dot{H}\dot{q} + S\dot{q} \right) d\tau - \int_0^t kJ^T(q(\tau))\Delta x(\tau) \, d\tau \\ = -H(q(t))\dot{q}(t) + H(q(0))\dot{q}(0) + \int_0^t \left(\frac{1}{2}\dot{H}\dot{q} - S\dot{q} \right) d\tau \\ - k\int_0^t J^T \Delta x \, d\tau, \quad (33)$$

which leads to:

$$\|C\Delta q(t)\| \leqslant \|H(t)\dot{q}(t)\| + \|H(t)\dot{q}(0)\| + \int_0^t \left\|\frac{1}{2}\dot{H}\dot{q} - S\dot{q}\right\| d\tau + k \int_0^t \|J^{\mathrm{T}}\Delta x\| d\tau, \tag{34}$$

where $\Delta q = q - q_{\mathrm{d}}$. Here we use symbol $H(t) = H(q(t))$ for abbreviation and in some cases omit descriptions of independent variable t or τ. Since $C \geqslant C^2 > 4H(q)$ for all q, (34) can be reduced to:

$$\|q(t) - q(0)\|_K \leqslant \frac{1}{2\sqrt{2}}\|C\Delta q(t)\|$$

$$\leqslant \frac{1}{2}\left\{\frac{1}{\sqrt{2}}\|H(t)\dot{q}(t)\| + \frac{1}{\sqrt{2}}\|H(0)\dot{q}(0)\|\right\}$$

$$+ \frac{1}{2\sqrt{2}}\int_0^t \dot{q}^{\mathrm{T}}\bar{C}\dot{q}\,d\tau + \frac{\sqrt{k}}{4}\int_0^t \sqrt{\frac{k}{2}\Delta x^{\mathrm{T}}\Delta x}\,d\tau, \tag{35}$$

where the second inequality comes from Appendix A. Further, according to $(1/\sqrt{2})\|H(q)\dot{q}\| \leqslant (1/2)\sqrt{K}$, (35) is reduced to:

$$\|\Delta q(t)\|_K \leqslant \frac{1}{4}\left(\sqrt{K(t)} + \sqrt{K(0)}\right) + \frac{\beta}{2\sqrt{2}}E(0)$$

$$+ \frac{\sqrt{2}}{2}\int_0^t \sqrt{3E(0)}\exp\left\{-\frac{9}{40}\tau\right\}d\tau$$

$$\leqslant \left(\frac{1}{2} + \frac{20\sqrt{6}}{9}\right)\sqrt{E(0)} + \frac{\beta}{2\sqrt{2}}E(0), \tag{36}$$

where β is at most of $O(10^{-1})$ as shown in Appendix A. Thus, if $r_1 \leqslant r_0/8$, $\|q^0 - q(0)\|_K \leqslant r_0/8$ and $E(0) \leqslant r_1^2$, then:

$$\|q(t) - q^0\|_K \leqslant \|q^0 - q(0)\|_K + \|q(t) - q(0)\|_K$$

$$< \frac{r_0}{8} + \left(\frac{1}{2} + \frac{20\sqrt{6}}{9}\right)r_0/8 + \frac{\beta r_1^2}{2\sqrt{2}} < \frac{r_0}{8} + \frac{6r_0}{8} + \frac{r_0}{8}$$

$$\leqslant r_0. \tag{37}$$

Thus, by setting $\varepsilon_1 = \min\{r_0/8, \delta_1\}$ and $r_1 = r_0/8$, it has been proved that any solution of (5) starting from $(q(0), \dot{q}(0))$ lying in $N^8(\varepsilon_1, r_1)$ remains in $N^8(\varepsilon_1, r_0)$ and asymptotically tends to $M_2 \cap N^8(\varepsilon_1, r_0)$. $\qquad\square$

4. SHORT-RANGE REACHING

Even in the case of short-range reaching motion such that $\|x(0) - x_{\mathrm{d}}\| = 0.05$–$0.15$ m, the proof of Theorem 1 is valid and ensures the convergence of joint motion $q(t)$ to some equilibrium state $(q^\infty, \dot{q} = 0) \in M_2 \cap N^8(\varepsilon_1, r_0)$. However, in

this case the metric norm $\|q - q(0)\|_K$ is not adequate for evaluating the change of $\Delta q(t)[= q(t) - q(0)]$ during the transient process of reaching motion in order to ensure that there is no possibility of occurrence of self-motion incurred from the joint redundancy as pointed out by Seraji [34]. In order to prove that the final posture q^∞ does not go far from the initial posture $q(0)$ like the posture 'C)' of Fig. 2 starting from the posture 'B)', it is necessary to introduce the Euclid metric $\|q(t) - q(0)\|$ or $\|C^{1/2}(q(t) - q(0))\|$. In reality, it is quite difficult to obtain a good estimate on the value of $\|q(t) - q(0)\|$. Hence, we evaluate an estimate of $\|C^{1/2}(q(t) - q(0))\|$ during maneuvering the robot arm by assuming that the arm is set at a still state at the initial time, i.e. $(q(0), \dot{q}(0) = 0) \in N^8(\varepsilon_1, r_0)$. To do this, consider the transformation of q and $\dot{q}$ to p and $\dot{p}$ defined as:

$$C^{1/2}\dot{q} = \dot{p}, \quad C^{1/2}q = p,$$

and the transformed Lagrange equation:

$$\bar{H}\ddot{p} + \left(\frac{1}{2}\dot{\bar{H}} + \bar{S}\right)\dot{p} + \dot{p} + k\bar{J}^{\mathrm{T}}\Delta x = 0, \tag{38}$$

instead of (5), which is obtained by multiplying (5) by $C^{-1/2}$ from the left and defining:

$$\begin{cases} \bar{H}(p) = C^{-1/2}H(q)C^{-1/2}, & \bar{J}(p) = J(q)C^{-1/2} \\ \bar{S}(p, \dot{p}) = C^{-1/2}S(q, \dot{q})C^{-1/2}. \end{cases} \tag{39}$$

In what follows we will give an upper bound on $\|p(t) - p(0)\|$ $(= \|C^{1/2}(q(t) - q(0))\|)$ based on another example of illustrative control under the following data on damping coefficients:

$$c_{11} = c_{22} = 1.00 \quad \text{and} \quad c_{33} = c_{44} = 0.160, \tag{40}$$

and the target and initial position:

$$\begin{cases} x(0) = -0.072 \text{ m}, & y(0) = 0.395 \text{ m} \\ x_{\mathrm{d}} = -0.150 \text{ m}, & y_{\mathrm{d}} = 0.300 \text{ m}, \end{cases} \tag{41}$$

where $\|x(0) - x_{\mathrm{d}}\| = \|\Delta x(0)\| = 0.1229$ m. Actually, computer simulation by using the initial posture $q(0) = [\pi/4, 7\pi/18, \pi/3, 5\pi/18]^{\mathrm{T}}$ (rad), which is the same as that used in simulation results of Figs 4–6, results in Figs 8–11. Although the damping factors c_3 and c_4 for the third and fourth joints (q_3 and q_4) are chosen fairly large, and therefore movements of these two joints become rather stiff, the endpoint of the robot arm converges to the target point x_{d} smoothly if the gain k is chosen around $k = 8.0$. Further, we observed by this simulation a noteworthy phenomenon that the smallest eigenvalue of $\bar{J}(p)\bar{J}^{\mathrm{T}}(p)$ becomes considerably larger than that of $J(q)J^{\mathrm{T}}(q)$ as shown in Fig. 11. This means that, by comparing Figs 11 and 7, $J(q)J^{\mathrm{T}}(q) \geqslant 0.08I_2$, but $\bar{J}(p)\bar{J}^{\mathrm{T}}(p) \geqslant 0.175I_2 > (1/6)I_2$ during maneuvering the robot arm. Since in this case of short-range reaching the endpoint
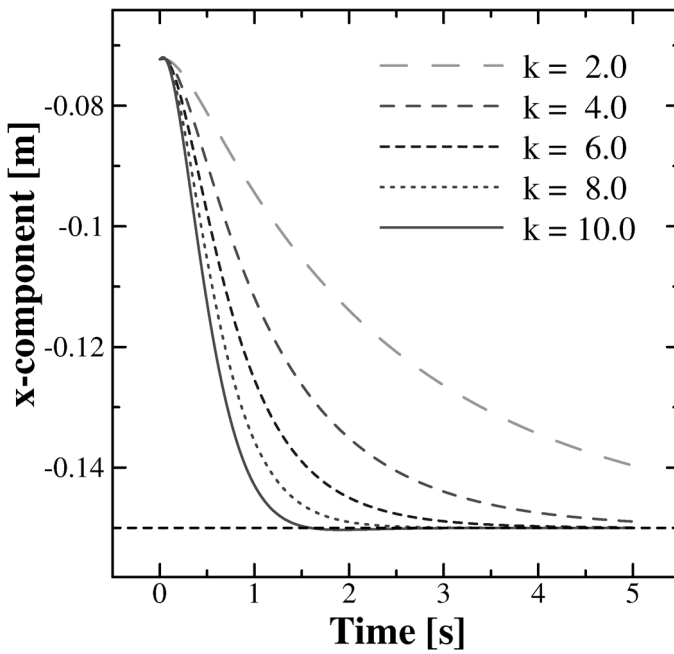
Figure 8. Transient responses of x when $c_1 = c_2 = 1.0$ and $c_3 = c_4 = 0.16$.
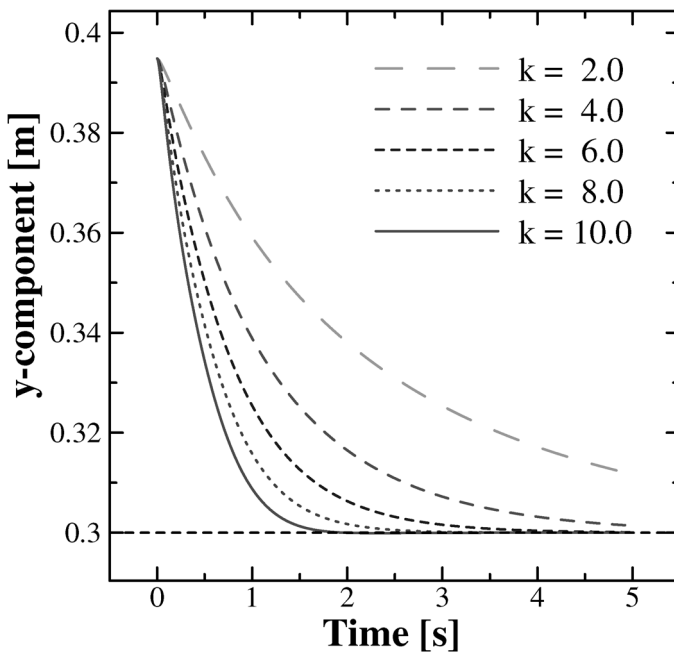
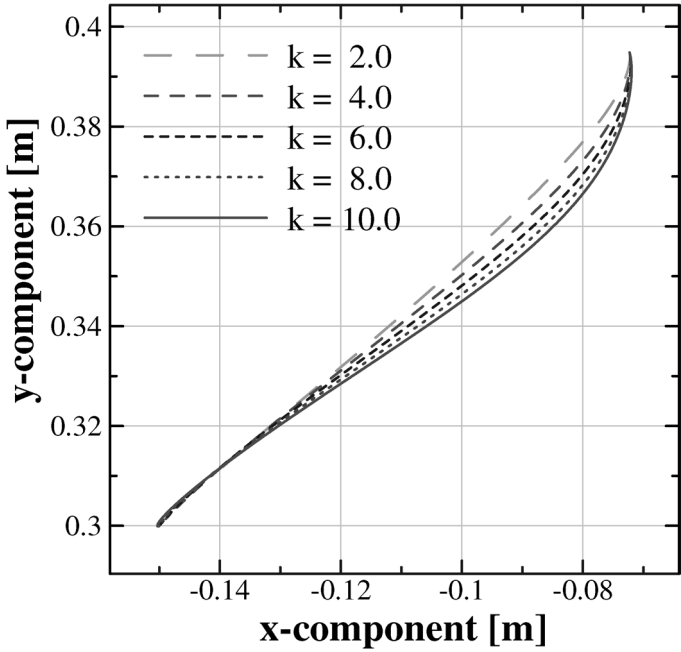**Figure 9.** Transient responses of y when $c_1 = c_2 = 1.0$ and $c_3 = c_4 = 0.16$.

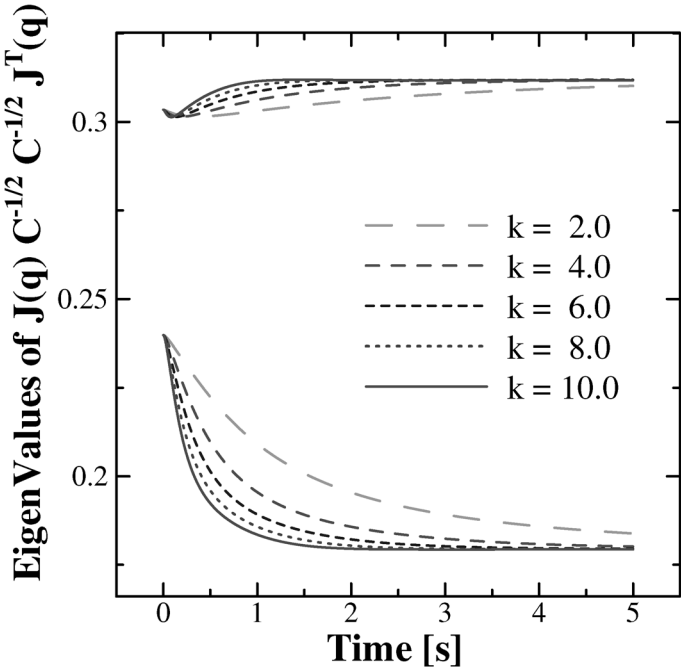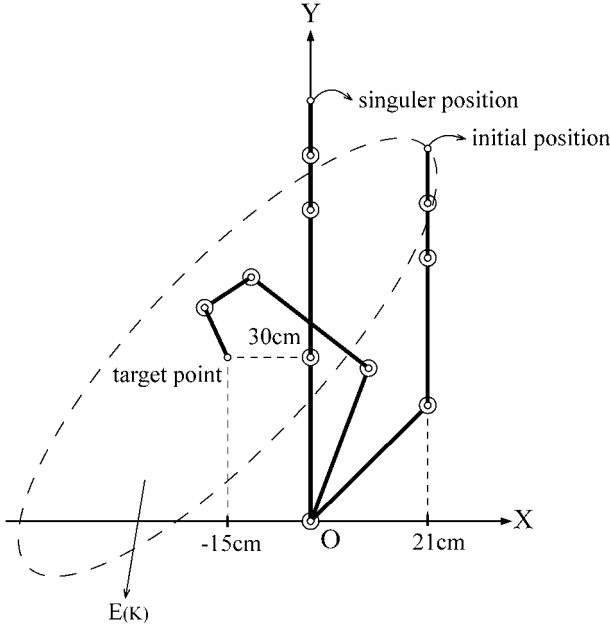**Figure 10.** Endpoint trajectory in the xy-plane when $c_1 = c_2 = 1.0$ and $c_3 = c_4 = 0.16$.

Figure 11. Behaviors of eigenvalues of $\bar{J}\bar{J}^T = JC^{-1/2}C^{-1/2}J^T$ when $c_1 = c_2 = 1.0$ and $c_3 = c_4 = 0.16$.

Figure 12. Reaching in global movement.

motion is confined to the circle $\|\Delta x(t)\| \leqslant \|\Delta x(0)\| = 0.1229$ m according to (6) and $\dot{q}(0) = 0$, it must be possible to show theoretically that $\bar{J}(p)\bar{J}^{\mathrm{T}}(p) \geqslant (1/6)I_2$ for all p inside $\|x - x_{\mathrm{d}}\| < 0.1229$ m because any posture whose endpoint is inside the circle $\|x - x_{\mathrm{d}}\| < 0.1229$ m is considerably different from the singular posture $q_2 = q_3 = q_4 = 0$ as seen in Fig. 12. However, in this paper we rather focus on the derivation of an upper bound on $\|p(t) - p(0)\|$ without presenting a rigorous proof on the inequality $\bar{J}(p)\bar{J}^{\mathrm{T}}(p) \geqslant (1/6)I_2$.

Now, for the sake of avoiding troublesome expressions of mathematical formulae, we omit the symbol "$\bar{\ }$" (bar) on $H,\ S$ and J, in (38) as shown in the following form:

$$H(p)\ddot{p} + \left(\frac{1}{2}\dot{H}(p) + S(p,\,\dot{p})\right)\dot{p} + \dot{p} + kJ^{\mathrm{T}}(p)\Delta x = 0. \tag{42}$$

At the same time we frequently omit writing the variables p and $\dot{p}$ in $H(p)$, $J(p)$, $S(p,\,\dot{p})$, etc., as far as no confusion arises. First, let us multiply (42) by $(\dot{p} + \alpha kJ^{\mathrm{T}}\Delta x)^{\mathrm{T}}$ from the left. Then, it follows that:

$$\frac{\mathrm{d}}{\mathrm{d}t}\left(\frac{1}{2}\dot{p}^{\mathrm{T}}H\dot{p} + \frac{k}{2}\Delta x^{\mathrm{T}}\Delta x + \frac{\alpha k}{2}\Delta x^{\mathrm{T}}\Delta x\right) + \dot{p}^{\mathrm{T}}\dot{p} + \alpha k^2\Delta x^{\mathrm{T}}JJ^{\mathrm{T}}\Delta x$$

$$+ \alpha k\Delta x^{\mathrm{T}}JH\ddot{p} + \alpha k\Delta x^{\mathrm{T}}J\left(\frac{1}{2}\dot{H} + S\right)\dot{p} = 0. \tag{43}$$

This can be rewritten in the form:

$$\frac{d}{dt}\left[\left\{\frac{1}{2}(\dot{p}+\alpha k J^{\mathrm{T}}\Delta x)^{\mathrm{T}}H(\dot{p}+\alpha k J^{\mathrm{T}}\Delta x)\right\}\right.$$
$$\left.+\frac{k}{2}\Delta x^{\mathrm{T}}\left\{(1+\alpha)I_2-\alpha^2 kJHJ^{\mathrm{T}}\right\}\Delta x\right]$$
$$+\|\dot{p}\|^2+\alpha k^2\Delta x^{\mathrm{T}}JJ^{\mathrm{T}}\Delta x+\alpha k h(\Delta x,\dot{p})=0, \tag{44}$$

where:

$$h(\Delta x,\dot{p})=\Delta x^{\mathrm{T}}J\left(-\frac{1}{2}\dot{H}+S\right)\dot{p}-\Delta x^{\mathrm{T}}\dot{J}H\dot{p}-\dot{p}^{\mathrm{T}}J^{\mathrm{T}}JH\dot{p}. \tag{45}$$

Since $\dot{J}$ is also linear in $\dot{p}$ and homogeneous in $\dot{p}$, the scalar function h of (45) is quadratic in $\dot{p}$. Therefore, and by virtue of the bound on $\|\Delta x\|$ as $\|\Delta x(t)\|<0.1229$, it follows from Appendix C that:

$$|h(\Delta x,\dot{p})|\leqslant\|\Delta x(0)\|\gamma_0\|\dot{p}\|^2+\gamma_1\|\dot{p}\|^2, \tag{46}$$

where $\gamma_0\leqslant 1/15$ and $\gamma_1\leqslant 1/12$.

Now, let us choose $\alpha=1.0$ and note the following inequality:

$$-k^2\Delta x^{\mathrm{T}}JJ^{\mathrm{T}}\Delta x=-\frac{1}{2}(\dot{p}+kJ^{\mathrm{T}}\Delta x)^{\mathrm{T}}H(\dot{p}+kJ^{\mathrm{T}}\Delta x)+\frac{k^2}{2}\Delta x^{\mathrm{T}}JHJ^{\mathrm{T}}\Delta x$$
$$+\frac{1}{2}\dot{p}^{\mathrm{T}}H\dot{p}+k\Delta x^{\mathrm{T}}JH\dot{p}-k^2\Delta x^{\mathrm{T}}JJ^{\mathrm{T}}\Delta x. \tag{47}$$

Since $H(p)<(1/4)I_4$ as discussed in Appendix C and:

$$k\Delta x^{\mathrm{T}}JH\dot{p}=\left(\frac{k}{\sqrt{2}}\Delta x^{\mathrm{T}}JH^{1/2}\right)\left(\sqrt{2}H^{1/2}\dot{p}\right)\leqslant\frac{k^2}{4}\Delta x^{\mathrm{T}}JHJ^{\mathrm{T}}\Delta x+\dot{p}^{\mathrm{T}}H\dot{p}, \tag{48}$$

(47) is reduced to:

$$-k^2\Delta x^{\mathrm{T}}JJ^{\mathrm{T}}\Delta x=-W(\dot{p},\Delta x)+k\Delta x^{\mathrm{T}}\Delta x-k^2\Delta x^{\mathrm{T}}JJ^{\mathrm{T}}\Delta x$$
$$+\frac{1}{2}\dot{p}^{\mathrm{T}}H\dot{p}+k\Delta x^{\mathrm{T}}JH\dot{p}$$
$$\leqslant-W(\dot{p},\Delta x)-k\Delta x^{\mathrm{T}}\left(kJJ^{\mathrm{T}}-I_2-\frac{k}{4}JHJ^{\mathrm{T}}\right)\Delta x$$
$$+\frac{3}{2}\dot{p}^{\mathrm{T}}H\dot{p}, \tag{49}$$

where:

$$W(\dot{p},\Delta x)=\frac{1}{2}(\dot{p}+kJ^{\mathrm{T}}\Delta x)^{\mathrm{T}}H(\dot{p}+kJ^{\mathrm{T}}\Delta x)+k\Delta x^{\mathrm{T}}\left(I_2-\frac{k}{2}JHJ^{\mathrm{T}}\right)\Delta x. \tag{50}$$

Thus, by referring to inequalities of (46) and (49), (44) when $\alpha = 1.0$ can be reduced to:

$$\frac{\mathrm{d}}{\mathrm{d}t} W(\dot{p}, \Delta x) = -\|\dot{p}\|^2 - k^2 \Delta x^{\mathrm{T}} J J^{\mathrm{T}} \Delta x - kh(\Delta x, \dot{p})$$

$$\leqslant -W(\dot{p}, \Delta x) - \frac{1}{2}\dot{p}(I_4 - 3H)\dot{p}$$

$$- k\Delta x^{\mathrm{T}} \left(kJJ^{\mathrm{T}} - I_2 - \frac{k}{4}JHJ^{\mathrm{T}}\right) \Delta x$$

$$+ (\gamma_1 + \gamma_0 \|\Delta x(0)\|)\|\dot{p}\|^2 - \frac{1}{2}\|\dot{p}\|^2. \tag{51}$$

In this case, we choose $k = 8.0$ and $\|\Delta x(0)\| \leqslant 0.1229$ m. Then, as discussed previously, $J(p)J^{\mathrm{T}}(p) \geqslant (1/6)I_4$ and furthermore $H(p) \leqslant (1/4)I_4$ and $JHJ^{\mathrm{T}} \leqslant (1/16)I_2$ (the details of these discussions are given in Appendix C). Thus, (51) can be reduced to:

$$\frac{\mathrm{d}}{\mathrm{d}t} W(\dot{p}, \Delta x) \leqslant -W(\dot{p}, \Delta x). \tag{52}$$

It should be noted at this stage that $W(\dot{p}, \Delta x)$ is positive definite in $\dot{p}$ and Δx when $k = 8.0$ because the inequality $JHJ^{\mathrm{T}} \leqslant (1/16)I_2$ leads to:

$$W(\dot{p}, \Delta x) = \frac{1}{2}(\dot{p} + kJ^{\mathrm{T}}\Delta x)^{\mathrm{T}} H(\dot{p} + kJ^{\mathrm{T}}\Delta x) + k\Delta x^{\mathrm{T}} \left(I_2 - \frac{k}{2}JHJ^{\mathrm{T}}\right) \Delta x$$

$$\geqslant \frac{1}{2}(\dot{p} + kJ^{\mathrm{T}}\Delta x)^{\mathrm{T}} H(\dot{p} + kJ^{\mathrm{T}}\Delta x) + \frac{3}{4}k\|\Delta x\|^2, \tag{53}$$

and the right-hand side is positive definite in $\dot{p}$ and Δx. Thus, it can be concluded from (52) that:

$$W(t) = W(\dot{p}(t), \Delta x(t)) \leqslant W(0)\mathrm{e}^{-t}, \tag{54}$$

with $W(0) = W(0, \Delta x(0)) = k\|\Delta x(0)\|^2$, which implies from (54) that:

$$\|\Delta x(t)\|^2 \leqslant \frac{4}{3}\|\Delta x(0)\|^2 \mathrm{e}^{-t}, \tag{55}$$

or equivalently:

$$\|\Delta x(t)\| \leqslant (2/\sqrt{3})\|\Delta x(0)\|\mathrm{e}^{-(1/2)t}. \tag{56}$$

We are now in a position to evaluate $\|p(t)\|$ $(= \|C^{1/2}(q(t) - q(0))\|)$. By taking the integral of (42) over time interval $[0, t]$, we obtain:

$$p(t) - p(0) = -k \int_0^t J^{\mathrm{T}}(p(\tau))\Delta x(\tau)\,\mathrm{d}\tau - H(p(t))\dot{p}(t) + \int_0^t \left(\frac{1}{2}\dot{H} - S\right)\dot{p}(\tau)\,\mathrm{d}\tau, \tag{57}$$

from which it follows that:

$$\|p(t) - p(0)\| \leqslant k \int_0^t \left\{\Delta \boldsymbol{x}^{\mathrm{T}}(\tau) J J^{\mathrm{T}} \Delta \boldsymbol{x}(\tau)\right\}^{1/2} \mathrm{d}\tau + \left\{\dot{p}^{\mathrm{T}}(t) H(p) H(p) \dot{p}(t)\right\}^{1/2}$$

$$+ \int_0^t \beta_1 \|\dot{p}(\tau)\|^2 \, \mathrm{d}\tau. \tag{58}$$

As discussed in detail in Appendix C, $H(p) \leqslant (1/4)I_4$, $\beta_1 \leqslant 1/10$ and the maximum eigenvalue of $J(p)J^{\mathrm{T}}(p)$ is less than $1/3$ as seen in Fig. 12, (58) is reduced to:

$$\|p(t) - p(0)\| \leqslant \frac{k}{\sqrt{3}} \int_0^t \|\Delta \boldsymbol{x}(\tau)\| \, \mathrm{d}\tau + \frac{1}{2} E(0) + \beta_1 E(0). \tag{59}$$

Then, by virtue of (56), we obtain:

$$\|p(t) - p(0)\| \leqslant \frac{k}{\sqrt{3}} \cdot \frac{2}{\sqrt{3}} \int_0^t \|\Delta \boldsymbol{x}(0)\| \mathrm{e}^{-\tau/2} \, \mathrm{d}\tau + \left(\frac{1}{2} + \beta_1\right) E(0)$$

$$\leqslant \frac{4k}{3} \|\Delta \boldsymbol{x}(0)\| + \left(\frac{1}{2} + \beta_1\right) E(0). \tag{60}$$

In the case of the illustrative example of a starting position given in (41), $\|\Delta \boldsymbol{x}(0)\| = \|\boldsymbol{x}(0) - \boldsymbol{x}_{\mathrm{d}}\| = 0.1229$, $k = 8.0$ and $E(0) = (k/2)\|\Delta \boldsymbol{x}(0)\|^2 = 4 \times 0.1229^2$, which leads to

$$\|p(t) - p(0)\| \leqslant \frac{32}{3} \times 0.1229 + 4\left(\frac{1}{2} + \frac{1}{10}\right) \times 0.1229^2$$

$$\leqslant 1.35 \text{ rad}. \tag{61}$$

It is also possible to obtain more detailed information about each upper bound on $|p_i(t) - p_i(0)| (= c_i|q_i(t) - q_i(0)|)$, $i = 1, 2, 3$ and 4, by using (58). Since $J(p)$ is expressed component-wise as:

$$J(p) = \left(\frac{\partial \boldsymbol{x}}{\partial q_1}, \frac{\partial \boldsymbol{x}}{\partial q_2}, c_3^{-1/2} \frac{\partial \boldsymbol{x}}{\partial q_3}, c_4^{-1/2} \frac{\partial \boldsymbol{x}}{\partial q_4}\right)$$

$$|q_1(t) - q_1(0)| \leqslant k \int_0^t \left\|\frac{\partial \boldsymbol{x}}{\partial q_1}\right\| \cdot \|\Delta \boldsymbol{x}\| \, \mathrm{d}\tau + \left(\frac{1}{2} + \beta_1\right) E(0)$$

$$|q_4(t) - q_4(0)| = \frac{1}{0.4}|p_4(t) - p_4(0)|$$

$$\leqslant \frac{k}{0.16} \int_0^t \left\|\frac{\partial \boldsymbol{x}}{\partial q_4}\right\| \cdot \|\Delta \boldsymbol{x}\| \, \mathrm{d}\tau + \left(\frac{1}{2} + \beta_1\right) E(0). \tag{62}$$

Since the 2D vectors $\partial \boldsymbol{x}/\partial q_1$ and $\partial \boldsymbol{x}/\partial q_4$ are expressed as:

$$\partial \boldsymbol{x}/\partial q_1 = (-y, x)^{\mathrm{T}}, \quad \partial \boldsymbol{x}/\partial q_4 = (-l_4 s_{1234}, l_4 c_{1234})^{\mathrm{T}},$$

as seen in (8) and (9) and the robot endpoint is inside the circle $\|\Delta x\|^2 < 0.1229^2$, it is possible to see that:

$$\left\| \frac{\partial x}{\partial q_1} \right\| \leqslant 0.5 \quad \text{and} \quad \left\| \frac{\partial x}{\partial q_4} \right\| = l_4 = 0.1.$$

Hence:

$$|q_1(t) - q_1(0)| \leqslant \frac{k}{2} \cdot \frac{2}{\sqrt{3}} \cdot \int_0^t \|\Delta x(0)\| e^{-\tau/2} \, d\tau + 4 \left(\frac{1}{2} + \beta_1 \right) \times 0.1229^2$$

$$\leqslant \frac{16}{\sqrt{3}} \times 0.1229 + 0.0363$$

$$\equiv 1.1305 + 0.0363 = 1.1668 \leqslant \frac{7}{18}\pi \text{ rad} \leqslant 70°, \tag{63}$$

$$|q_4(t) - q_4(0)| \leqslant \frac{k}{0.16} \times 0.1 \times \frac{2}{\sqrt{3}} \int_0^t \|\Delta x(0)\| e^{-\tau/2} \, d\tau$$

$$+ 4 \left(\frac{1}{2} + \beta_1 \right) \times 0.1229^2$$

$$= \frac{20}{\sqrt{3}} \times 0.1229 + 0.0363$$

$$= 1.4554 < \frac{\pi}{2} \text{ rad} = 90°. \tag{64}$$

Another upper bound on $|q_2(t) - q_2(0)|$ and $|q_3(t) - q_3(0)|$ can be obtained in a similar way. Finally, these results claim that, under the choice of damping coefficients of (40) together with $k = 8.0$, there does not arise any unnecessary self-motion like the posture of 'C)' shown in Fig. 2 during the transient behavior of each joint motion, if the starting point is given in (41) and the posture is given by setting $q(0) = [45.0, 70.0, 60.0, 30.0]^T$ (deg).

5. REACHING WITH GLOBAL MOVEMENT

In the case of reaching with global movement when $\|\Delta x(0)\|$ is larger than 0.15 m, the problem of evaluation of upper bounds on joint motions becomes quite difficult or impossible. For example, consider the initial posture ($q_1 = \pi/4$, $q_2 = \pi/4$, $q_3 = q_4 = 0$) (rad) as shown in Fig. 12 and the control problem of moving the robot arm endpoint toward the target posture $x_d = (-0.15, 0.3)$ m. In this case, the initial posture is close to the singular posture that satisfies $q_2 = q_3 = q_4 = 0$. That is, singularity of $J(q)J^T(q)$ arises if and only if $q_2 = q_3 = q_4 = 0$. Nevertheless, it is possible to confirm that the same set of damping coefficients $\{c_1 = 1.0, c_2 = 0.6, c_3 = 0.1, c_4 = 0.04\}$ as of (20) yields a good performance of this type of global reaching for the choice of the stiffness gain around $k = 8.0$ as shown in Figs 13–15, although the initial value of the smallest eigenvalue of
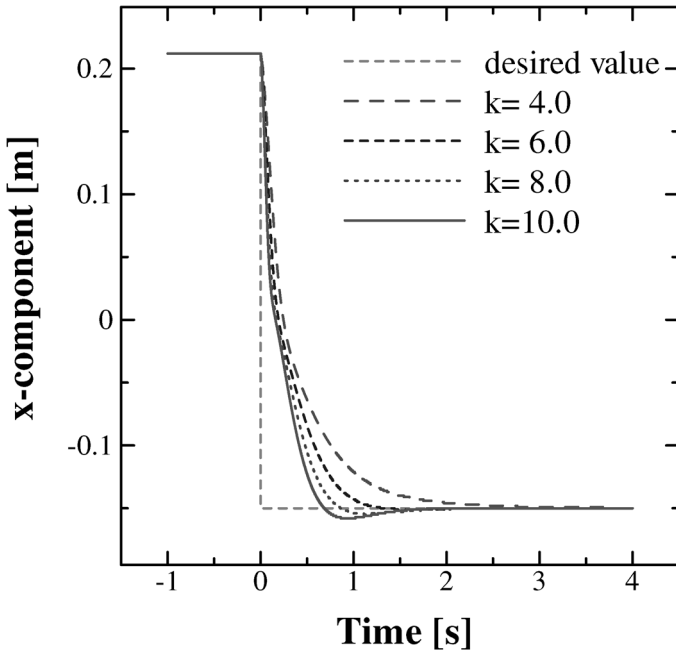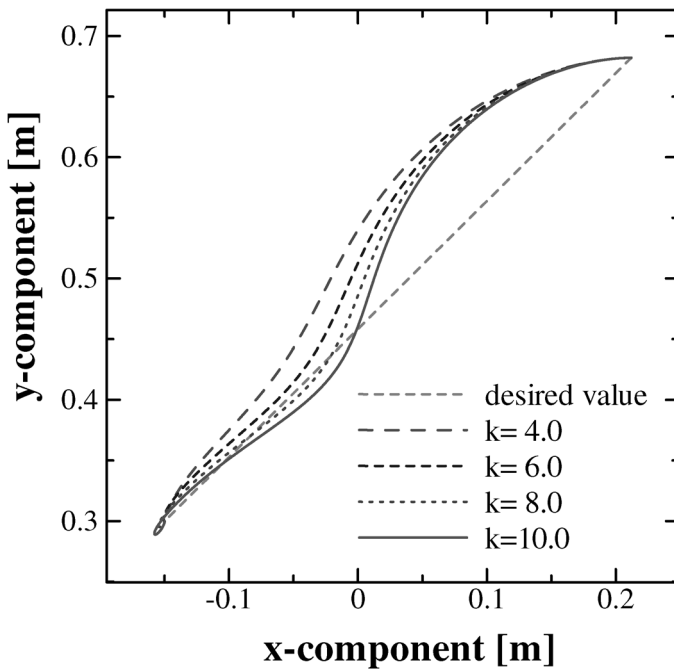
Figure 13. Transient responses of x of the global reaching starting from the initial posture shown in Fig. 9.

$J(q)J^T(q)$ appears to be very small around $t = 0.0$ as seen in Fig. 16 and compared with Fig. 7. It should be noted that to control the motion of a robot arm whose posture is lying in the vicinity of its Jacobian singularity is not an easy problem even in the case that the robot arm is non-redundant and hence $J(q)$ is square. However, to control the robot arm to quickly leave the initial posture with Jacobian singularity by using the task-space PD feedback with the transpose of its Jacobian matrix is practically feasible because it is possible to verify that all components of $J^T(q)(x - x_d)$ become minus at the singularity position ($q_1 = \pi/2$, $q_2 = q_3 = q_4$) shown in Fig. 12 if x_d is located on the left side of the arm. That is, in this case the motion starts with zero velocity $\dot{q}(0) = 0$ and all positive joint angle accelerations $\ddot{q}_i(0) > 0$ for $i = 1, \ldots, 4$. This means that the arm starts to move so as to increase all joint angles, and, in particular, turn the values of $q_2(t)$, $q_3(t)$ and $q_4(t)$ positive, and consequently increase the smallest eigenvalue of $J(q)J^T(q)$ quickly as seen in Fig. 16. Therefore, it would be possible to ascertain that the robot endpoint moves quickly toward a neighborhood sphere of x_d with some appropriate radius $r = 0.10$–0.15 m and reaches the circle within 1 s or so. Once the endpoint reaches such a neighborhood circle of x_d with radius $r = 0.10$–0.15 m, it is already ascertained that the robot endpoint will remain in the sphere by using the same control law and converge to the target point x_d without incurring much self-motion of redundant joints. Therefore, it remains important to show theoretically that the control scheme based on (2) enables movement of the robot arm toward a neighborhood sphere
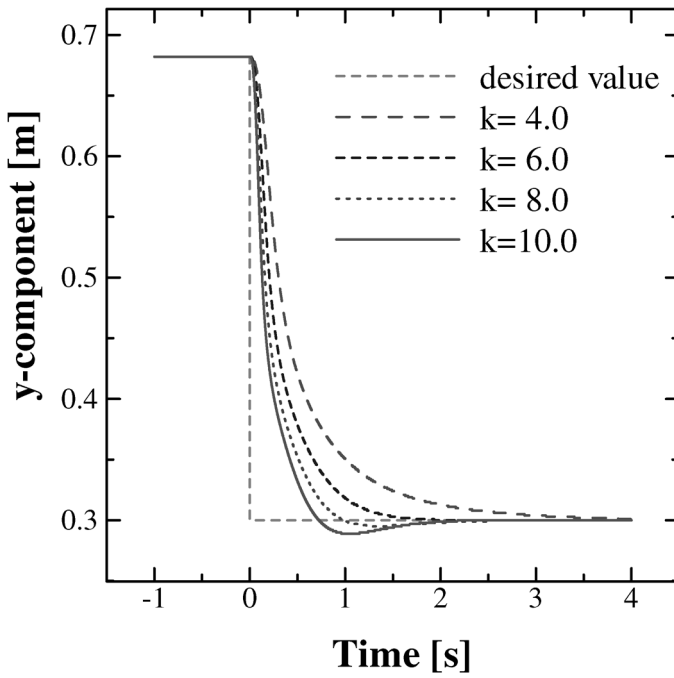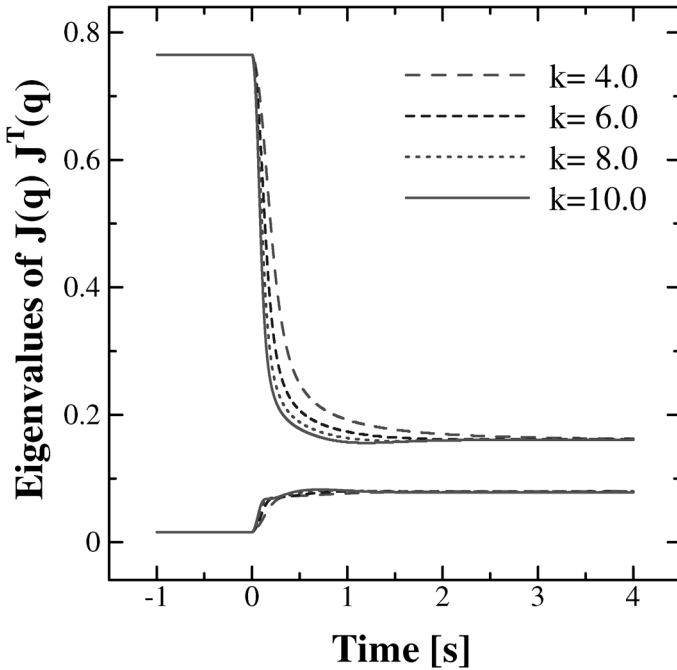
Figure 14. Transient responses of y for various k.

Figure 15. Movement of the arm endpoint in the xy-plane.

**Figure 16.** Transient responses of two eigenvalues of $J(q)J^T(q)$.

with radius $r = 0.10$–0.15 m by choosing an appropriate stiffness parameter k and an appropriate combination of damping gains c_i, $i = 1, \ldots, 4$. This problem will be treated more in theoretical detail in a future work.

6. COMPARISONS BETWEEN HUMAN REACHING AND ROBOTIC REACHING

According to Latash [35], the characteristics of human reaching are summarized as:

 (i) Endpoint trajectory is close to a straight line from the starting point to the target.
 (ii) Endpoint velocity profile becomes bell-shaped.
(iii) Endpoint acceleration has double peaks.
(iv) Joint angle trajectories, angular velocities and angular accelerations may become different in each joint.

He also pointed out that the most noteworthy 'reproducibility' of skilled human reaching is 'non-reproducibility' of joint motion trajectories. This is called 'variability', which is seen typically even in repeated motions played by golfers and professional athletes. However, variability of the endpoint is low relative to that of each joint motion. Such variability of each joint motion in repeated reaching trials may be produced by the variability of coordinated 'synergy' of motions between joints
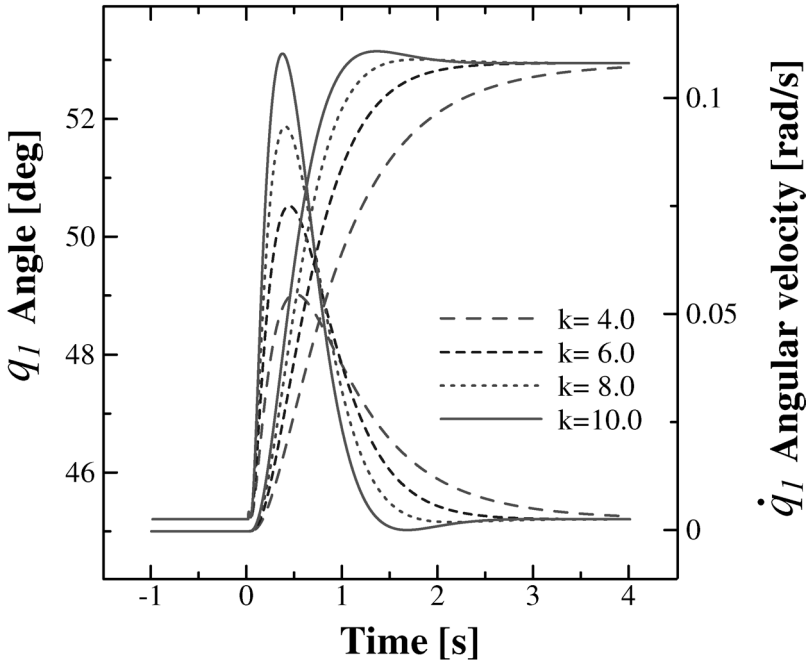
Figure 17. Transient responses of joint angle q_1 and angular velocity $\dot{q}_1$ corresponding to Figs 4–7.

in the case of humans, as claimed by Latash [35]. In contrast, this variability of joint motion can be easily seen in robotic reaching by changing damping coefficients in joint control signals. In fact, changing the synergy of damping coefficients from $(c_1 = 1.0, c_2 = 0.6, c_3 = 0.1, c_4 = 0.04)$ to $(c_1 = c_2 = 1.0, c_3 = c_4 = 0.16)$ incurs much change in the behavior of joint motions, in particular joint $q_4(t)$. In the former case $q_4(t)$ moves from $q_4(0) = 50°$ to $q_4(\infty) = 42.5°$, but in the latter case it only moves from $q_4(0) = 50°$ to $q_4(\infty) = 46°$. In contrast, the motions of the first two joints do not change much between these two cases.

It seems rather difficult to choose an appropriate set of damping factors c_i $(i = 1, \ldots, 4)$ that nearly actualize the straight line property of movement of the endpoint. This difficulty can be easily predicted by observing the two simulation results on xy-plane profiles of the endpoint motions in Figs 6 and 15, whose trajectories in the xy-plane are considerably different and, in particular, differ in the starting directions around $t = 0$ for the fixed set of damping factors. This means that the best set of damping factors must be chosen depending on the starting position and posture so as to actualize the straight line property of the endpoint motion. In those cases, endpoint velocities $\dot{x}$ and $\dot{y}$ do not show a bell-shaped profile. However, the bell-shaped property of joint angular velocities $\dot{q}_i(t)$ can be realized in robotic reaching as shown in Figs 17 and 18. The profile of the endpoint speed $v = (\dot{x}^2 + \dot{y}^2)^{1/2}$ actually becomes bell shaped.

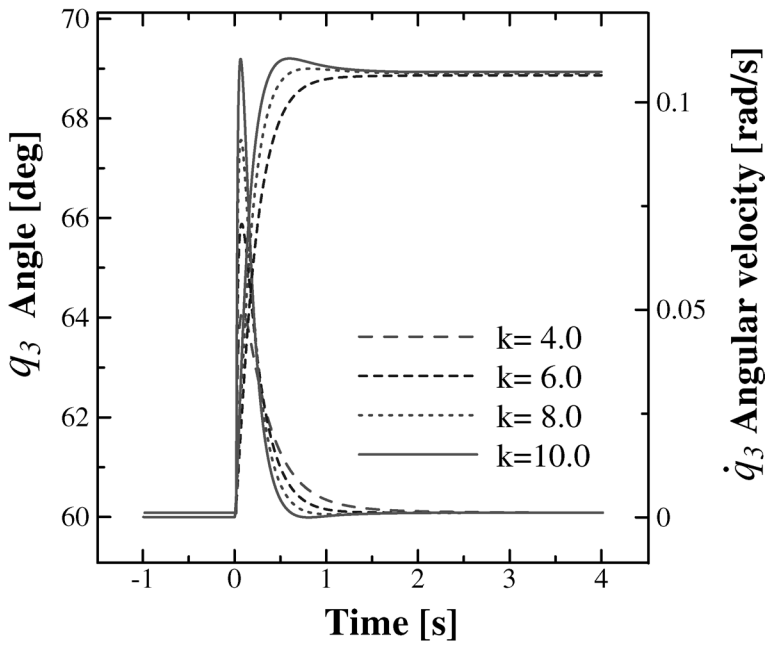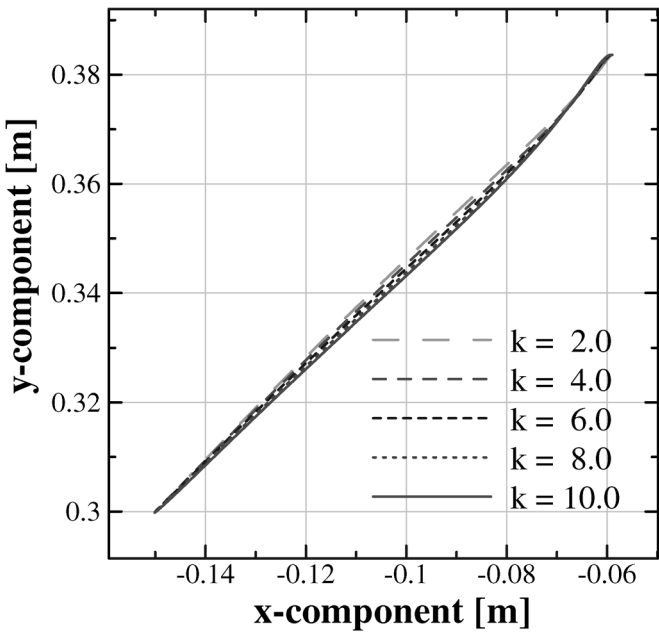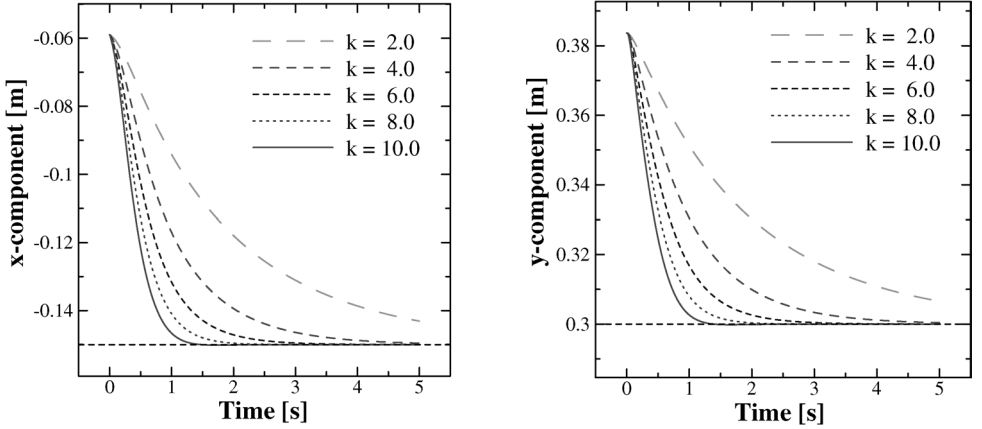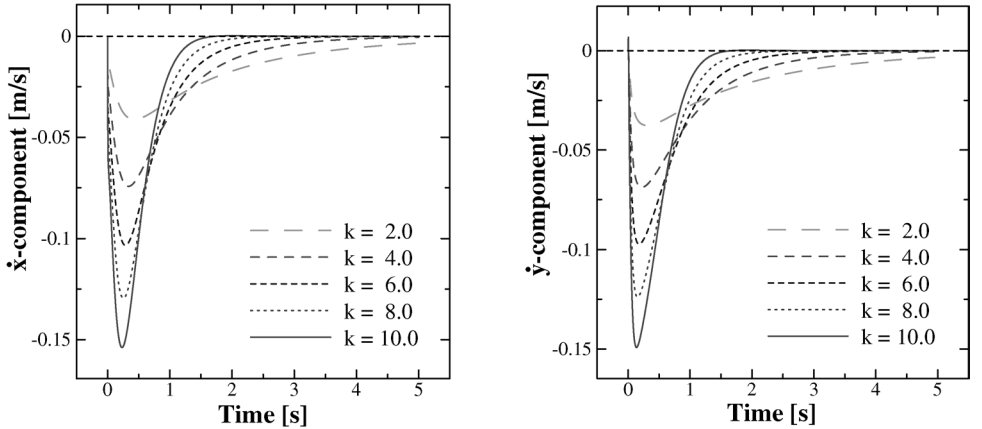**Figure 18.** Transient responses of joint angles q_3 and angular velocity $\dot{q}_3$.

Figure 19. Endpoint trajectory of short-range reaching when the control of (2) is used with $c_1 = 1.35$, $c_2 = 0.60$, $c_3 = 0.108$, $c_4 = 0.030$.

Figure 20. Transient responses of endpoint coordinates x and y.

Figure 21. Transient responses of endpoint velocities $\dot{x}$ and $\dot{y}$.

Through many trials of computer simulation of robotic reaching, like human infants trying to reach objects and repeating such practices, we found a better set of damping factors together with a posture with pre-shaping in the following way:

(i) C is approximately equivalent to $3.0 \times H^{1/2}(0)$, i.e. $c_1 = 1.35$, $c_2 = 0.60$, $c_3 = 0.108$, $c_4 = 0.030$

(ii) $q(0) = [45, 70, 60, 60]^{\mathrm{T}}$ (deg)

In this case the approximately straight line trajectory of the endpoint movement has been realized as shown in Fig. 19. At the same time, each time history of $\dot{x}$ and $\dot{y}$ behaves like a bell-shaped profile as shown in Figs 20 and 21, although each slope of $\dot{x}$ and $\dot{y}$ becomes rather gentle after $t = 1.0$ to $t = \infty$ in comparison with that at the rising time immediately after $t = 0.0$. This phenomenon must be easily improved by re-adjusting damping factors by increasing them when the endpoint is approaching close to a target. In this case, the initial posture of the finger link

(the fourth link) given by $q(0)$ of (ii) is pre-shaped so as to point straight to the target. This pre-shaped posture makes the forth component of $kJ^T(q)\Delta x$, which is expressed as $k(\partial x/\partial q_4)^T\Delta x$, vanish at the initial time $t = 0.0$. In other words, if the posture of the finger link is pre-shaped before starting the reaching motion so as to point toward the target and the set of damping coefficients is chosen adequately, then typical reaching movements similar to human reaching and characterized by items (i)–(iv) above can be actualized by using a redundant multi-joint robot without introducing any performance index to resolve inverse kinematics. It should be noted that the most important characteristics of human skilled motion pointed out by Latash [35] as 'variability' can be handled with the mathematical definitions of 'stability on a manifold' and 'transferability to a submanifold'.

7. CONCLUSIONS

This paper has shown that human-like multi-joint reaching movements can be actualized by using a redundant degrees of freedom planer robot and a simple feedback scheme from task space to joint space with linear joint angular velocity feedback without resolving inverse kinematics and introducing any artificial performance index. This result supports the EP hypothesis concerning human motor control proposed by Feldman [21] and Bizzi *et al.* [17] even in the case of excess degrees of freedom reaching movements. At the same time, it is possible to claim that the proposed theoretical analysis and simulation results point to the importance of the coordinated synergistic choice of effective damping factors among joints rather than the 'generation' of potential functions that exert spring-like forces on joints. Although this paper assumes that all joints can be directly controlled by actuators differently from the case of human reaching exerted by a group of muscles and tendons, the obtained results present some of the implications of the importance of modeling of 'viscous-like' dynamics of the neuromuscular system effective as damping forces at the slowing down stage of reaching motion. This aspect has not yet been discussed in the literature of robotics research or in the physiological literature, except for a series of papers by Hogan (e.g., Ref. [36]), where inter-relationships among mobility tensors of a set of joints and the endpoint and stiffness tensors through the Jacobian matrix are explored, but any quantitative effects of viscouse-like force terms on the differential equation of motion (Lagrange's equation) have not yet been fully analyzed.

REFERENCES

1. J. Lenarcic (Ed.), Special Issue on Redundant Robots. *Lab. Robotics Automat.* **6**(1) (1991).
2. Y. Nakamura, *Advanced Robotics: Redundancy and Optimization*. Addison-Wesley, Reading, MA (1991).
3. T. Yoshikawa, Manipulability of robotic mechanisms, *Int. J. Robotics Res.* **4**, 3–9 (1984).

4. O. Khatib, A unified approach for motion and force control of robot manipulators: The operational space formulation, *IEEE J. Robotics Automat.* **3**, 43–53 (1987).

5. J. M. Hollerbach and K. C. Suh, Redundancy resolution of manipulators through torque optimization, *IEEE J. Robotics Automat.* **3**, 308–316 (1987).

6. V. Potkonjak, S. Tzafestas, D. Kostic, G. Djoudjevic and M. Rasic, The handwriting problem, *IEEE Robotics Automat. Mag.* **March**, 35–46 (2003).

7. H. Hanafusa, T. Yoshikawa and Y. Nakamura, Analysis and control of articulated robot arm with redundancy, in: *Proc. 8th IFAC Triennial World Congr.*, Kyoto, pp. 1927–1932 (1981).

8. Y. Nakamura and H. Hanafusa, Task priority based redundancy control of robot manipulators, in: *Robotics Research: The Second International Symposium*, H. Hanafusa and H. Inoue (Eds), pp. 447–456. MIT Press, Cambridge, MA (1985).

9. J. Baillieul, Avoiding obstacles and resolving kinematic redundancy, in: *Proc. IEEE Int. Conf. on Robotics and Automation*, San Francisco, CA, pp. 1698–1704 (1986).

10. D. E. Whitney, Resolved motion rate control of manipulators and human protheses, *IEEE Trans. Man–Machine Syst.* **10**, 47–53 (1969).

11. A. Liegeois, Automatic supervisory control of the configuration and behavior of multi-body mechanism, *IEEE Trans. Syst. Man Cybernet.* **7**, 868–871 (1977).

12. N. Bernstein, *The Coordination and Regulation of Movements*. Pergamon, London (1967).

13. H. T. A. Whiting (Ed.), *Human Motor Actions — Bernstein Reassessed*. Elsevier Science, Amsterdam (1984).

14. R. M. Murray, Z. Li and S. S. Sastry, *A Mathematical Introduction to Robotic Manipulation*. CRC Press, Boca Raton, FL (1994).

15. G. Hinton, Some computational solutions to Bernstein's problems, in: *Human Motor Actions — Bernstein Reassessed*, H. T. A. Whiting (Ed.), pp. 413–438. Elsevier Science, Amsterdam (1984).

16. A. G. Feldman, Once more on the equilibrium-point hypothesis (λ model) for motor control, *J. Motor Behav.* **18**, 17–54 (1986).

17. E. Bizzi, A. Polit and P. Morasso, Mechanisms underlying achievement of final head position, *J. Neurophys.* **39**, 435–444 (1976).

18. T. Flash and N. Hogan, The coordination of arm movements: an experimentally confirmed mathematical model, *J. Neurosci.* **5**, 1688–1703 (1985).

19. A. P. Georgopoulos, On reaching, *Annu. Rev. Neurosci.* **9**, 147–170 (1986).

20. E. Bizzi, N. Hogan, F. A. Mussa-Ivaldi and S. Giszter, Does the nervous system use equilibrium-point control to guide single and multiple joint movements? *Behav. Brain Sci.* **15**, 603–613 (1992).

21. A. G. Feldman, Functional tuning of the nervous system with control of movement or maintenance of a steady posture. III. Mechanographic analysis of the execution by man of the simplest motor tasks, *Biophysics* **11**, 766–775 (1966).

22. N. Hogan, An organizing principle for a class of voluntary movements, *J. Neurosci.* **4**, 2745–2754 (1984).

23. W. Nelson, Physical principle for economies of skilled movements, *Biol. Cybernet.* **46**, 135–147 (1983).

24. Z. Hasan, Optimized movement trajectories and joint stiffness in unperturbed, initially loaded movements, *Biol. Cybernet.* **53**, 373–382 (1986).

25. Y. Uno, M. Kawato and R. Suzuki, Formation and control of optimal trajectory in human multijoint arm movement, *Biol. Cybernet.* **61**, 89–101 (1989).

26. M. Kawato, Y. Maeda, Y. Uno and R. Suzuki, Trajectory formation of arm movement by cascade neural network model based on minimum torque-change criterion, *Biol. Cybernet.* **62**, 275–288 (1990).

27. M. L. Latash (Ed.), *Control of Human Movement*. Human Kinetics, New York, NY (1994).

28. J. P. Scholz and G. Schöner, The uncontrolled manifold concept: identifying control variables for a functional task, *Exp. Brain Res.* **126**, 289–306 (1999).
29. S. Arimoto, P. T. A. Nguyen, H.-Y. Han and Z. Doulgeri, Dynamics and control of a set of dual fingers with soft tips, *Robotica* **18**, 71–80 (2000).
30. S. Arimoto, K. Tahara, J.-H. Bae and M. Yoshida, A stability theory of a manifold: concurrent realization of grasp and orientation control of an object by a pair of robot fingers, *Robotica* **21**, 163–178 (2003).
31. S. Arimoto, M. Yoshida, J.-H. Bae and K. Tahara, Dynamic force/torque balance of 2D polygonal objects by a pair of rolling contacts and sensory–motor coordination, *J. Robotic Syst.* **20**, 517–537 (2003).
32. S. Arimoto, Intelligent control of multi-fingered hands, *Annu. Rev. Control* **28**, 75–85 (2004).
33. S. Arimoto, *Control Theory of Nonlinear Mechanical Systems: A Passivity-based and Circuit-theoretic Approach*. Oxford University Press, Oxford (1996).
34. H. Seraji, Configuration control of redundant manipulators: theory and implementation, *IEEE Trans. Robotics Automat.* **5**, 472–490 (1989).
35. M. L. Latash, *Neurophysiological Basis of Movement*. Human Kinetics, New York, NY (1998).
36. N. Hogan, The mechanics of multi-joint posture and movement control, *Biol. Cybernet.* **52**, 315–331 (1985).

APPENDIX A

It is easy to check that every entry of $H(q)$, $H_{ij}(q)$, is independent of q_1 and principal inertia moments I_1 to I_4 appear in $H(q)$ as constants. Hence, the possibly biggest terms in $H(q)$ associated with $\cos(q_i)$, $i = 1, 2, 3, 4$, are $2m_2 l_1 s_2 \cos q_2$ in $H_{11}(q)$ and $m_2 l_1 s_2 \cos q_2$ in $H_{12}(q)$ or $H_{21}(q)$, where s_2 signifies the length between the second joint (elbow) center to the mass center of the second link. According to Table 1:

$$2m_2 l_1 s_2 = 2 \times 0.7634 \times 0.3 \times 0.135$$
$$= 0.0618.$$

Thus, $\dot{q}_1$ appears in $\dot{q}^T((1/2)\dot{H} + S)J^T \Delta x$ as a cross term of $\dot{q}_1 \dot{q}_2 \sin(q_2)$ with at most the coefficient 0.0618. Since:

$$|2m_2 l_2 s_2 \dot{q}_1 \dot{q}_2 \sin(q_2)| \leqslant \frac{1}{2}m_2 l_2 s_2 \dot{q}_1^2 + 2m_2 l_2 s_2 \dot{q}_2^2, \tag{A.1}$$

$\bar{c}_1$ can be chosen at most as $\bar{c}_1 = 0.0155$ and $\bar{c}_2$ is $O(0.0618)$. Other upper bounds on the coefficient of cross terms $\dot{q}_1 \dot{q}_3$ and $\dot{q}_1 \dot{q}_4$ can be evaluated similarly, which are proportional to m_3 and m_4, respectively. Thus, it is possible to ascertain that $\bar{c}_1$ to $\bar{c}_4$ can be chosen in the ranges:

$$\bar{c}_1 \leqslant 0.005, \quad \bar{c}_2 \leqslant 0.2, \quad \bar{c}_3 \leqslant 0.05, \quad \bar{c}_4 \leqslant 0.01. \tag{A.2}$$

It is also possible to verify by referring to the ranges of $H_{ij}(0)$ from Table 2 and (20) that:

$$C \geqslant 4\left(H(q) + \frac{2}{7}\bar{C}\right). \tag{A.3}$$

APPENDIX B

Since the singular-valued decomposition of J is equivalent to J^{T}, the spectral radius of J^{T} is the same as J. However, as the maximum eigenvalue of $J(q)J^{\mathrm{T}}(q)$ is always less than 0.24 according to Fig. 7 and, in particular, is going to decrease toward around 0.18, it may be possible to ascertain theoretically that $\lambda_{\max}(J^{\mathrm{T}}(q)J(q)) < 0.25$ during maneuvering the robot starting from the initial position given in Table 2. However, the rigorous proof is mathematically sophisticated and therefore omitted. Fortunately, a more rigorous proof of Theorem 1 without assuming or proving this bound on λ_{M} is given in Section 4.

APPENDIX C

Since the most dominant entry of $H(q)$ is $H_{11}(q)$, the second dominant one is $H_{22}(q)$ and, furthermore, the first submatrix $J_1(p)$ of $J(p) = [J_1(p), J_2(p)]$ is equivalent to $J_1(p) = \bar{J}_1(q) = J_1(q)$ because of selection of $c_1 = c_2 = 1.0$, the spectral radius λ_{M1} of the submatrix $J_1^{\mathrm{T}}J_1H_{11}$ is about $\lambda_{\mathrm{M1}} = 0.0625 = 1/16$, where:

$$H = \begin{bmatrix} H_{11} & H_{12} \\ H_{21} & H_{22} \end{bmatrix}, \quad J^{\mathrm{T}}J = \begin{bmatrix} R_{11} & R_{12} \\ R_{21} & R_{22} \end{bmatrix}. \tag{C.1}$$

In addition to this $J_1^{\mathrm{T}}J_1H_{11}$, there is another contribution $J_1^{\mathrm{T}}J_2H_{21}$, but the spectral radius of this 2×2 matrix is small relative to λ_{M1} because each entry of $\bar{H}_{21}(p)$ is relatively small [at most of $O(10^{-2})$]. Hence, the spectral radius of $J^{\mathrm{T}}JH$ can be evaluated as $\lambda_{\mathrm{M}}(J^{\mathrm{T}}JH) \leqslant 1/12$ and hence:

$$\dot{p}J^{\mathrm{T}}(p)J(p)H(p)\dot{p} \leqslant \frac{1}{12}\|\dot{p}\|^2. \tag{C.2}$$

In a similar way to this, it possible to evaluate the following:

$$J(p)H(p)J^{\mathrm{T}}(p) \leqslant \frac{1}{12}I_2. \tag{C.3}$$

ABOUT THE AUTHORS

Suguru Arimoto received the BS degree in Mathematics from Kyoto University, Japan in 1959 and the DE degree in Control Engineering from the University of Tokyo, Japan in 1967. From 1959 to 1961 he was with Oki Electric Industry Co. Ltd, Tokyo, as an Engineer in the Electric Computer Department. From 1962 to 1967 he was a Research Assistant and from 1967 to 1968 Lecturer in the Department of Mathematical Engineering and Information Physics, a University of Tokyo. In 1968 he joined the Faculty of Engineering Science at Osaka University, Osaka, Japan, as an Associate Professor and in 1973 he was promoted to Professor of Systems Engineering. In 1988 he was invited to join the University of Tokyo as Professor of the Department of Mathematical Engineering and Information Physics. In 1997 he

retired from the University of Tokyo and moved to Ritsumeikan University, where he contributed to the establishment of a new department. Since 1997 he has been Professor in the Department of Robotics. His research interests are in information theory, control theory, cybernetics, robotics and machine intelligence. He is an IEEE Fellow (1983), IEICE Fellow (2000) and RSJ Fellow, and was awarded the National Medal with a Purple Ribbon from the Japanese Government in 2000 and the IEEE Third Millennium Medal from the IEEE in 2000.

Masahiro Sekimoto received the BS degree in Robotics from Ritsumeikan University, Japan in 2003. Since 2003, he has been a Masters student in the Department of Robotics, Ritsumeikan University. His research interests include redundant robots, robotic fingers, cybernetics and biomimetics.

Hiroe Hashiguchi received the BS and MS degrees in Robotics from Ritsumeikan University in 2001 and 2003, respectively. Since 2003, he has been a Doctoral student in the Department of Robotics, Ritsumeikan University, Japan. His research interests include redundancy resolution, sensory feedback control and handwriting robot.

Ryuta Ozawa received the BS degree in Precision Engineering, and MS and PhD degrees in Mechanical Engineering from Meiji University in 1996, 1998 and 2001, respectively. He was a Research Assistant at the University from 1999 to 2002. In 2002, he worked as a Research Fellow of the Japan Society for the Promotion of Science at the University. He is currently a Lecturer at Ritsumeikan University. His current interests include tendon-driven mechanisms, elastic joint robots, robotic fingers, impedance control and redundant robots.